國立臺灣大學理學院心理學研究所

碩士論文

Graduate Institute of Psychology

College of Science

National Taiwan University

Master Thesis

初級感覺皮質內興奮性神經元之可塑性誘導：

大鼠觸鬚模型

Guided Neuroplasticity of Excitatory Neurons in Primary

Sensory Cortex: A Whisker Model

鄭宇博

Yu-Po Cheng

指導教授：葉俊毅 博士

Advisor: Chun-I Yeh, Ph.D.

中華民國 109 年 1 月

January 2020

國立台灣大學理學院心理學研究所

論文口試委員會審定書

鄭宇博 先生所提論文 初級感覺皮質內興奮性
神經元之可塑性誘導：大鼠觸鬚模型

經本委員會審議， 符合碩士學位標準， 特此證明。

論文考試委員會

主席 吳玉威

委員 吳玉威　　　裴育晟

梁庚辰　　　葉俊毅

_____　_____

指導教授： 葉俊毅

所主任： 周泰立

中華民國 109 年 1 月 7 日

致謝

大學部即將畢業時，雖打算過出國進修或進入業界，然而考量到實驗實作經驗不足、與業界銜接的技能也還不成熟，也或許心底的理由是想繼續待在棒球校隊拼全國冠軍，我透過了推甄申請進入了心理學研究所。起初我期望從電生理研究中精進學術能力與程式編寫，取得攻讀海外博士的門票，但這個目標在漫漫的三年半時間中載浮載沉。值得感謝的是，研究所階段中我得到了許多人的支持與幫助，如今研究總算告一段落，而對於未來的迷惘也有所減少。

能夠順利完成研究所學業以及這篇研究，我最感謝的是無條件支持我的父母和家人。從小到大，父母總是不遺餘力地將資源投入在我和弟弟的教育上，雖然我總是不情願參加課後安親班、補習班等等活動，但我知道這是父母期望我們兄弟能過得比他們更好、生活更豐富，而犧牲其他花費甚至個人興趣所換來的。升上高中、大學乃至於現階段的研究所，父母讓我自由選擇，也總默默關切並給予心靈與經濟上的支持，我真的真的很感謝父母為我付出的一切。

碩士班的求學階段，最重要的莫過於實驗的經驗與能力，以及資料分析、結果闡述的技巧，更甚者則能對研究室留下貢獻。感謝台大的相余學長、威翔學長、威銘學長、思毅學長、戴聞學長和欽益學長，看著他們報告期刊研究、個人實驗進度到最後的學位口試，都讓我對於學術討論有更深更廣的理解。而與他們的討論、相處及請益，也是我研究所回憶中精彩的時光。也特別感謝林口長庚的吉麟學長、宇銘學長、亭仔學姐、美嬋學姐及詳鵬學長，在動物實驗、程式編纂以及院內各樣繁複流程的貼心指教，沒有你們的支持這篇研究簡直無從開始。最後，我深深地感謝黃建嘉學長、裴育晟老師和葉俊毅老師，謝謝您們一路以來的指導與關愛。從初入研究室的一知半解開始，到中期實驗失敗或陷入低潮，及最後衝刺完成論文，謝謝您們與我一起思索該如何詮釋資料與改進研究，更傾囊相授學術經驗和待人處世哲理，使我能從不同以往的角度檢視研究與生活。可惜我在研究室留下的貢獻並不多，只希望沒有留下太多困擾，非常感謝老師們的提攜與包容。

此外，擔任口試委員的梁庚辰老師與吳玉威老師，對於本篇研究的完整度也扮演重要的角色，同時也提醒了我從更多面向去思考問題的可能。感謝老師們對於研究本身和未來方向的寶貴意見，期許這些養份能使我對知識的建構有更深刻而完整的理解，也謝謝兩位老師撥出時間協助我走過這道最終關卡。

　　最後要感謝碩士生生活中擔任我心靈食糧與負面情緒出口的同儕、台大棒球校隊成員與校友們，以及自大學時期伴我共同成長的女友。謝謝威辰、鴻揚和柏安這段時間的相互勉勵，雖然你們都比我早拿到文憑是有點過份，但很高興我們都完成了這個人生階段，期許未來的日子仍能成為彼此的動力。謝謝台大棒球隊的所有人，讓我有了一個學業外的歸宿，更認識了各種性格、各個領域的好夥伴，相信我們共同消磨的歲月會在未來展現它的光芒。感謝女友玟秀願意陪伴充滿傻勁卻又常自我懷疑的我，謝謝你一直擔任我的心靈支柱與忍受我的健忘，至今與未來的努力都將歸功於你。

摘要

神經可塑性研究過去多著眼於少數神經的突觸間權重變化，如神經活動時間相依可塑性（STDP）研究等，本研究則試圖探討大群神經的功能可塑性。我們使用結構上有良好對應關係（topography）的大鼠觸鬚、大腦皮質桶狀組織系統（whisker barrel system）做為研究模型，引入光遺傳學技術做刺激操弄，並參照神經活動時間相依可塑性之實驗流程，以不同時間間隔重複呈現光刺激和觸鬚物理刺激。觸鬚神經首先根據其反應特性來定義主要觸鬚（principal whisker, PW）與鄰近觸鬚（adjacent whisker, AW），在進行光刺激和物理刺激配對時僅撥動其一（PW or AW）。我們在大鼠的桶狀皮質區域（barrel field）進行胞外電生理記錄，藉由比較配對前與配對後神經活動改變來瞭解是否誘發可塑性。另外，大部分桶狀皮質內的神經都有方向性偏好（direction selectivity），故於配對時只選擇單一固定方向撥動觸鬚，來瞭解觸鬚方向偏好是否也具可塑性。我們針對對光刺激和兩根觸鬚刺激皆有反應的神經進行分析（$n = 168$），將近一半（$n = 82/168$）的神經在配對前後的反應有顯著改變，其改變的方向性（上升或下降）與神經在配對前能被誘發反應的機率呈現負相關。我們也發現配對觸鬚刺激的方向性和神經本身方向選擇性的相關會顯著影響可塑性：當配對神經主要觸鬚並在其偏好角度移動時，神經誘發反應會下降，而當配對神經主要觸鬚並在其偏好角度相反方向移動時，神經誘發反應反而會會提升。另外出乎我們意料，刺激配對中兩刺激的時間間隔對神經可塑性的程度及改變方向性沒有任何影響。綜合以上結果，光遺傳學技術可以在大鼠完整觸鬚皮質區產生神經可塑性，神經誘發反應改變的方向，與神經本身的反應機率，以及配對觸鬚移動的方向性有關，但是不受兩配對刺激間的時間與順序影響。

關鍵字: 桶狀皮質、電生理、神經可塑性、光遺傳學

Guided Neuroplasticity of Excitatory Neurons in Primary Sensory Cortex: A Whisker Model
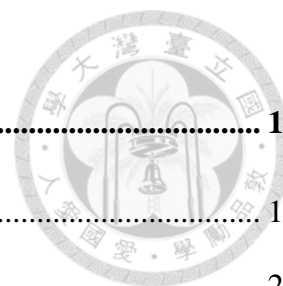
Yu-PO Cheng
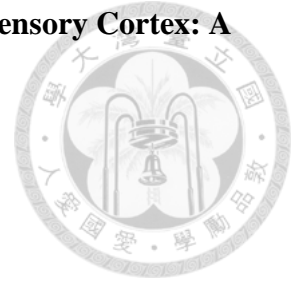
Abstract

Neuroplasticity, such as spike timing dependent plasticity (STDP), has been investigated primarily based on the change of synaptic weights among few neurons. In this research, we studied the functional plasticity in the topographically organized circuitry of rat whisker barrel system by manipulating activities in a large number of neurons. We hypothesized that, following the STDP rules, repetitive delivery of stimuli pairs in an intact brain could induce plasticity by altering response properties of single neurons such as firing rate and directional selectivity. We paired neural activities induced by stimulating a single whisker [principal whisker (PW) or adjacent whisker (AW)] with optogenetic stimulation (100 repeats) with different time delays between them. We recorded extracellularly from neurons in the cortical barrel corresponding to the principal whisker, and measured changes of neuronal activity before and after the parings. Directional selectivity for PW and AW deflections were measured separately by stimulating them in eight directions at 8 Hz before and after pairings. During the pairings, the chosen whisker (PW or AW) was deflected in a fixed direction in order to verify whether the paired direction was a determinant factor in neuroplasticity.

Among the 39% of neuronal population ($n = 168/430$) responded to both optical and physical (PW and AW) stimulation, almost half of them (49%, $n = 82/168$) shown significant changes in their mean firing rate after the optical-physical pairing. The change

of the firing rate is negatively correlated with the cell's original firing probability. Moreover, the difference between the neuron's original preferred direction and the paired direction has a strong effect on whether the neuron was upregulated or downregulated. In the PW-pairing condition, the mean response of PW was upregulated when the paired direction was opposite to the neuron's preferred direction, but was downregulated when the paired direction was the same as the neuron's preferred direction. To our surprise, the order and the duration between optical stimulation and physical stimulation has no effect on the amplitude and the direction of the change in firing rate. Overall, optical stimulation can induce neuroplasticity *in vivo* in intact barrel cortex. The change of the induced neuroplasticity by pairing physical and optical stimulations is related to the neuron's original firing probability and the deflecting direction of the paired whisker, but is not affected by the order and the timing between the two paired stimuli.
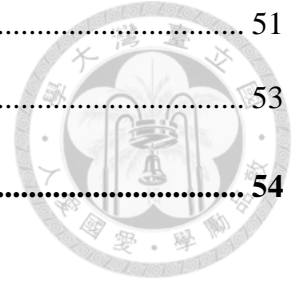
Table of Contents

List of Tables

List of Figures

1. Introduction

1.1. Somatosensory Cortex of Rodents

In the primary somatosensory cortex (S1) of rodents, the topographic organization at the cortical layer 4 was found and named "barrels" (Woolsey & Van der Loos, 1970). A single barrel column receives its primary input stemmed from mechanoreceptors within its corresponding whisker follicle and some inputs from adjacent whiskers (Le Cam, Estebanez, Jacob, & Shulz, 2011; Petersen, 2007; Simons, 1978; Wright & Fox, 2010). Because of the specificity in connections between the whisker and the barrel column, the whisker-barrel model has become a powerful tool in studying sensory processing and its underlying circuits including the horizontal connections between barrel columns and the feedforward connections between peripheral receptors and S1 neurons.

The barrel field is a general name of regions including barrel cortex (some researchers only referred layer 4 of barrel field as barrel cortex) and areas between barrels (septa) across cortical layers. Electrophysiology studies have shown that neurons in the barrel field manifested low firing rate (de Kock, Bruno, Spors, & Sakmann, 2007; Petersen, Hahn, Mehta, Grinvald, & Sakmann, 2003) and direction selectivity of external stimulus (Le Cam et al., 2011; Simons, 1978, 1983). Studies using adaptation (Heiss, Katz, Ganmor, & Lampl, 2008; Katz, Heiss, & Lampl, 2006; Khatri, Hartings, & Simons, 2004; Khatri & Simons, 2007; Maravall, Petersen, Fairhall, Arabzadeh, & Diamond, 2007), sensory deprivation (Feldman & Brecht, 2005; Jacob, Mitani, Toyoizumi, & Fox, 2017; Jacob, Petreanu, Wright, Svoboda, & Fox, 2012; Rasmusson, 1982), and current injection (Jacob, Brasier, Erchova, Feldman, & Shulz, 2007; Meliza & Dan, 2006) paradigms showed neuroplasticity could be induced within the rodent barrel field. However, little was known about whether the manipulation of the principal whisker might influence neuronal activity evoked by adjacent whiskers or *vice versa*. Most previous studies used only the neuron's optimal

1

stimulus but not suboptimal ones to study neuroplasticity. Here we proposed to study the neuroplasticity *in vivo* in adult barrel cortex by pairing whisker stimulation with optical stimulation, which tends to affect a large number of neurons simultaneously.
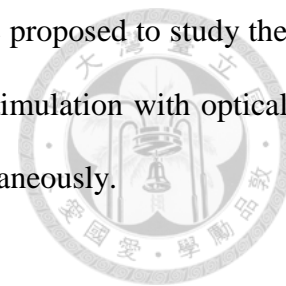
1.2. Neuroplasticity

Neurons might change their properties throughout the life time due to development, environment, experience, learning and even injury. In the sensory system, neurons encode external stimulus mainly based on corresponding patterns of evoked responses such as temporal coding (Butts et al., 2007; Engel, König, Kreiter, Schillen, & Singer, 1992; L. M. Jones, Depireux, Simons, & Keller, 2004; Singh & Levy, 2017) and frequency coding (Khatri et al., 2004; Maravall et al., 2007). Weinberger (1995) noted that it was once thought that sensory neuron's activity remained robust in order to faithfully represent external stimulus in the environment. However, some studies (Rasmusson, 1982; Van der Loos & Woolsey, 1973) reported that sensory system has the capability to show neuroplasticity even in the adult brain. Several paradigms have shown that the response features of sensory neurons can be manipulated by changing the synaptic weight between presynaptic and postsynaptic neurons (Khatri et al., 2004; Meliza & Dan, 2006; Van der Loos & Woolsey, 1973).

One critical feature of neuroplasticity is the order and the onset asynchrony between presynaptic and postsynaptic neurons. Hebb's rule (Hebb, 1949) was the first hypothesis to claim that when presynaptic activity was quickly followed by postsynaptic activity, the strength of the connection between the two neurons would be increased. Later in 1990s, Bi and Poo found that the synaptic weight of two connected cells could be altered according to the spike timing asynchrony: long-term potentiation (LTP) was found when presynaptic activity led and long-term depression (LTD) was found when postsynaptic activity led (Bi

2

& Poo, 1998). The bidirectional change in synaptic weighting (spike-time dependent plasticity, STDP) might be essential to the formation of topographic map and neuronal receptive fields. The STDP is also related to learning in mature neural circuits, such as sequential movements, reinforcement learning, and temporal difference learning.

The cellular mechanism for STDP was related to the NMDA receptor, metabotropic glutamate receptor (mGluR), and cannabinoid type 1 receptor (CB1R) (D. E. Feldman, 2012). The magnitude and time course of calcium influx through NMDA receptor determined whether LTP or LTD was produced. High concentration of internal calcium led to LTP while moderate concentration of internal calcium led to LTD, and no plasticity was found in low calcium condition.

1.3. Optogenetics Manipulation

Optogenetic technique is a powerful tool in study neuroplasticity because it could target a specific cell type to elicit or suppress neuronal activity with high temporal precision (Aravanis et al., 2007; Gunaydin et al., 2010; N. Li et al., 2011). There are two types of opsins: Type I opsins are found in prokaryotes, algae, and fungi, and Type II opsins are found in animal cells. Channelrhodopsin and halorhodopsin are widely used Type I opsins. The channelrhodopsin is a light-gated ion channel that allows cations like Na^+, K^+ and Ca^{2+} to pass the membrane; the halorhodopsin is a light-gated ion pump that specifically carries Cl^- into the cell. Thus, channelrhodopsin is used for depolarization and induction of neuronal activity, whereas halorhodopsin is used for polarization and suppression of neuronal activity.

Channelrhodopsin-induced responses were similar to current injection induced responses (Zhao et al., 2011) in cortical interneuron, dorsal striatum and brainstem of transgenic mice. In this study, we used channelrhodopsin in the barrel cortex to guide

3

neuroplasticity by affecting excitatory neurons expressing CaMKII. The adeno-associated virus (AAV) was used to carry channelrhodopsin and fluorescent protein (mCherry) into CaMKII expressing cells in the rat barrel cortex. When channelrhodopsin was stimulated by blue light, ion channels would open to allow inward cation current, which leads to depolarization and the production of action potentials. We also followed the STDP protocol by repetitively pairing physical stimulation and optical stimulation to induce neuroplasticity.

1.4. Aims of Present Study

In the present study, we studied the functional plasticity in the topographically organized circuitry of rat whisker barrel system by manipulating activities in a large number of neurons. We applied the STDP protocol by pairing physical stimulation (deflecting a whisker) with optical stimulation to see whether the physical-optical paring could lead to functional changes of individual neurons in the intact brain. We also manipulated the time between physical and optical stimulations to see whether the firing rate and directional preference of individual neurons might change according with the temporal manipulation. Results from the study could be helpful in evaluating the possibility and the limitation of neuroplasticity in the intact brain, which might be informative for future development of light-induced sensory function alteration or rehabilitation in the brain.

We hypothesized that the guided neuroplasticity of sensory function to the principal whisker might also change the responses evoked by adjacent whisker and vice versa. A neuron within the barrel field receives input not only from its principal whisker but also from its adjacent whisker. It is possible that manipulation on one whisker would alter responses evoked by other whiskers due to changes of signal recipient weightings.

4

Furthermore, we hypothesized that direction selectivity could also be altered by the physical-optical pairing. In the barrel cortex, neurons respond differently to whisker deflection in various directions. Although the deflection in the whisker's suboptimal direction might evoke relatively weak or no supra-threshold activities, the synaptic weighting has the potential to be enhanced or suppressed, which then could further lead to change of spiking activity. Finally, STDP was reported to be a dominant rule in *in vitro* conditions (Bi & Poo, 1998; Feldman, 2012; Meliza & Dan, 2006; Yao & Dan, 2001), whether the STDP rules can be applied in *in vivo* scenario was unclear, especially when optogenetic tools were introduced to directly elicit activity of a larger number of cortical neurons.

2. Materials and Methods
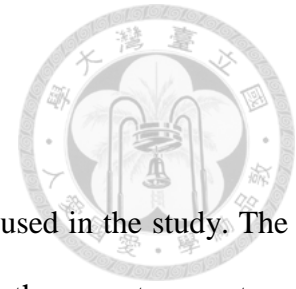
2.1. Subjects

Seventeen male adult Sprague Dawley rats (300-500 g) were used in the study. The animals were housed in a 12-h light/12-h dark circadian cycle under the room temperature between 22 °C to 25 °C. Food and water were available ad libitum. Animals were housed in group (2 animals per cage) until their weights were over 500 g.

2.2. AAV Virus Injection

Adeno-associated virus (AAV) were used to deliver channelrhodopsin onto excitatory neurons in the primary somatosensory cortex (S1, Fig. 1A). Animals were lightly anesthetized with isoflurane (3%) and then were injected intraperitoneally (i.p.) with the mixture of ketamine (100 mg/kg) and xylazine (10 mg/kg). To maintain steady anesthesia, one third of the dosage of the ketamine and xylazine mixture were delivered every half an hour. Animals' heads were shaved before surgery.

Stereotaxic surgery was performed to create a burr hole on the right part of skull (5 mm lateral and 2 mm posterior to the bregma). Analgesic (lidocaine ointment) was smeared on the scalp after sterilization. Incision were made from the midpoint of both eyes to the right posterior. Tissue on the top of skull was removed. A burr hole was made using a dental driller.

A microinjection syringe (Hamilton) was loaded with 0.7 µl of plasmid AAV9-CaMKII-hChR2(E123A)-mCherry-WPRE-hGH (Penn Vector Core). The first penetration would reach 1.8 mm in depth respective to the brain surface. After 10-minute-restoration of the brain, injection syringe would be pulled back to the 1.5 mm depth to the surface. After 5 minutes, microinjection started. The injection rate was 0.07 µl/min. After injection, we sutured the wound on the scalp and applied sterilization and analgesic. When animals

6

recovered from the anesthesia, they were transferred back to their home cages.
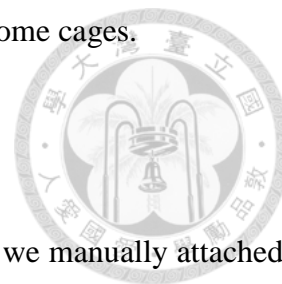
2.3. Electrophysiology Recording

In order to deliver light stimulation right at the recording site, we manually attached a tapered-tip optical fiber onto a single-shank multiple-channel silicon probe (Cambridge NeuroTech, E16 electrodes).

Isoflurane inhalation anesthesia was performed before intraperitoneally injection of urethane (1.4 g/kg), which was diluted in normal saline (1.4 g/ 3 cc). One third dosage of urethane were delivered every 3-4 hours to maintain stable anesthesia. Animals were then transferred onto the stereotaxic apparatus, disinfection and light lidocaine were applied at the surgical site on the shaved scalp. After removal the scalp, burr holes were drilled onto the left skull for head-fixation purpose, 3 screws were driven into the drilled holes with a grounding cable wired on them. After placement of screws, a copper pillar was placed between them. Dental cement was applied to fixate the pillar and screws. After 20-30 mins of dental cement fixation, craniotomy of a 4 by 4 mm^2 window centered at 5 mm lateral, 3 mm posterior to the bregma on the right hemisphere were performed with a dental driller. Pia mater was removed before recording electrodes penetration. The recording probe was held on the stereotaxic bar with an angle between 20 and 30 degrees from the vertical, so the probe was placed perpendicularly to the brain surface (Fig. 1B, left). Signals were amplified and high-pass filtered with a recording system (Blackrock microsystems, Cerebus) under a 30-kHz sampling rate.

2.4. Whisker Stimulation

The whiskers were trimmed to about 1 mm in length from the facial pad. Manual mapping of the principal whisker (receptive field) was conducted after recording probe

penetration. The principal whisker (PW) and one adjacent whisker (AW) (one of the surrounding whiskers that triggered the strongest response, mostly in the same arc) were inserted into the piezoelectric actuator based whisker stimulators, respectively. Trajectory of whisker deflection was a combination of asymmetric sine waves with a 9-ms forward and a 41-ms backward in one specific direction (there was a total of 8 different directions separated from each other by 45 degrees). The max amplitude of the whisker deflection was 150 μm. Blank trials were also included in the whisker stimulation session to measure spontaneous activity. In each whisker stimulation session, there were 20 repetitions of the 8 stimulation directions and 1 blank event. The order of the stimulation was pseudorandomly arranged.

Piezoelectric actuator (Noliac, NAC2710) based whisker stimulators were controlled by customized MATLAB programs (MathWorks). A computer sent digital signals controlled by MATLAB to current output modules (National Instruments, cDAQ 9263), which then delivered a direct current to an amplifier with desired voltage. The amplifier tripled input voltage and sent output signals to piezoelectric actuator based stimulator. There were two movable axes for each piezoelectric actuator, whose movable directions covered 360°. The piezoelectric actuator worked under a continuous 30 Volt current input and bended systematically according to another current input's voltage. For one whisker stimulator, two input channels for working power and other two input channels for movement control were needed. Thus, in order to perform deflection of PW and AW individually, we designed a customized MATLAB program sending 4 output channels for whisker deflection controlling signals and 1 output channel for timestamps of each stimulus onset and offset. Stimulus onset timestamps were transmitted to Blackrock recording system.

Another MATLAB program was designed for calibration of piezoelectric actuator

movements. The output voltage of current output modules gradually increased from 0 volt to 10 volts with a 0.05-volt step. A laser ranger (OMRON, ZX2-LD50), whose output signal was sent to the Blackrock recording system and was used to detect movement of piezoelectric actuator based stimulator's tip. By performing regression of input current voltage to the piezoelectric actuator and corresponding movement of stimulator's tip, we could then control desirable whisker deflection with gathered parameters.

2.5. Light Stimulation

A pilot study of a small unit set was performed to testify light stimulation evoked activity under various parameter sets. Light intensity were controlled at 2, 5 and 10 mW, and stimulation time window varied from 10, 20, 50, 100 ms.

Single units' responses to light stimulation was measured before the main experiment with 5-10 mW intensity and 50 ms duration. Light stimulation delivery was controlled by customized MATLAB programs. A computer sent digital signals to current output modules which then transmitted direct current to a laser shutter. The shutter was closed when there were no input signals, which made a blocked optical path from the light source (PSU-H-LED, MBL-F-473-200mW) to an output end of optical fiber stub (Hong Kong Plexon, ferrule fiber stubs) through a commercial optical fiber (Plexon). When direct current with voltage greater than 5 volts reached the laser shutter, it opened and allowed light stimulation delivered from the tip of output optical fiber. A copy of direct current signal was simultaneously sent to Blackrock recording system as the timestamp of stimulation onset and offset. There was only 1 output channel designed for abovementioned purpose in a customized MATLAB code.

2.6. Pairing Experiment

We measured physical evoked activity of PW and AW deflection before and right after pairing of physical and optical stimulation. There were 4 sessions of whisker stimulation for both the PW and the chosen AW before the pairing and 4 sessions after that (Fig. 1C). The inter-session-interval was 20 seconds for both intervals between two physical stimulation sessions, and that between physical stimulation session and pairing session.

In the pairing session, whisker stimulus and optical stimulus were delivered with a fixed time delay (Fig. 1D). Only one whisker was chosen to be deflected in one direction throughout the entire session. The trajectory of whisker deflection was the same with whisker stimulation, a morphed sinusoid wave with max amplitude of 150 μm. Light stimulation was 50-ms-width pulse (473 nm, 5-10 mW). Pairing repeated for 100 repetitions at 1 Hz frequency. Time delays between two stimulus onsets ranged from -40 – 40 ms.

Both physical and optical stimulation were controlled by a customized MATLAB program, which contained 4 output channels for piezoelectric actuator movement, 1 output channel for timestamp of whisker stimulation and 1 output channel for both shutter control and timestamp of light stimulation.

2.7. Offline Sorting

Offline sorting of single unit signals was done using Offline Sorter (Plexon) software. Raw data were first high pass filtered with the Butterworth 4 pole 250 Hz filter. A negative threshold would then either manually decided or set around 4-7 times of the standard deviation negatively. Signals passed the threshold would be scattered on 2D and 3D PCA panels (Fig. 3C, 5B) which were done by their spike waveform pattern (200 and 800 μs

10

before and after the intersection point of the raw data and the threshold). Single units were then defined under a 5-point rating protocol. Only the units higher than 3 points were considered as well isolated and been further analyzed. Rating protocol was as following:

(1): multi-units, artificial noises or no spikes at all.

(2): single-units, spikes that could not be clustered or containing zero point of PCA panel or mass center.

(3): single-units & clustered which not containing zero point of PCA panel or mass center.

(4): (3) & well isolated, visible boundaries.

(5): (4) & great distance from noises.

2.8. Data Analysis

Peristimulus timing histograms (PSTH) was calculated with 2-ms bin size. Onset latency and peak latency of whisker stimulation evoked responses were measured. The onset latency was defined as the first time bin of the two successive bins with amplitudes higher than 3 times of the standard deviation of the spontaneous activity. Peak latency was determined as the time bin with the maximum amplitude after onset latency. If peak latency was greater than 50 ms, the trial would be considered as an undetected trial.

Firing probability was calculated as number of trials with evoked activity over total trial number in one physical stimulus session. For instance, a neuron responded to physical stimulus for 4 times within 20 repetitions, its firing probability would be 0.2. Stimulus evoked firing rate was calculated as average number of spikes within 50-ms-window after onset latency. Firing rate was standardized by subtraction with baseline activity, which was the average number of spikes within 50-ms-window in blank trials, in order to estimate manipulation effect at the population level.

Pairing success rate was defined as the percentage of success pairs in pairing session. When there was at least one spike within 30-ms time window after stimulus onset for both optical and physical stimulus, the trial was considered as a success pair. For instance, if there were 20 success pairs within 100 pairs, the success rate was 0.2.
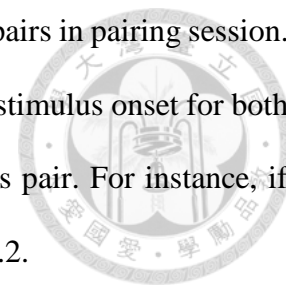
Stepwise linear multiple regression models were constructed using MATLAB regression learner APP. Independent variables (predictors) were tested whisker identity (PW or AW), pairing condition (PW pairing or AW pairing), SOA, firing probability before pairing, paired direction and interaction term between any two of these factors (one-on-one). Eight dependent variables (responses) were fitted separately, which were firing rate change of preferred direction, firing rate change index of preferred direction, firing rate change of paired direction, firing rate change index of paired direction, mean firing rate change, mean firing rate change index, spontaneous firing rate change, and spontaneous firing rate change index.

2.9. Histology

Paraformaldehyde perfusion was performed after experiment. Coronal brain slices of 50 µm thickness (Fig. 2) were cut by freezing microtome at -20 °C. The infected cells expressed channelrhodopsin would also express fluorescent mCherry, which could be directly observed under fluorescence microscopy and captured by a CCD camera. Anterior-posterior position was then determined by comparing landmark structure such as hippocampus, ventricles and subcortical structures etc. with rat brain atlas. Infection range of AAV vector was then estimated by boundary of visible mCherry expressing cell body in the neocortex (Fig. 3).
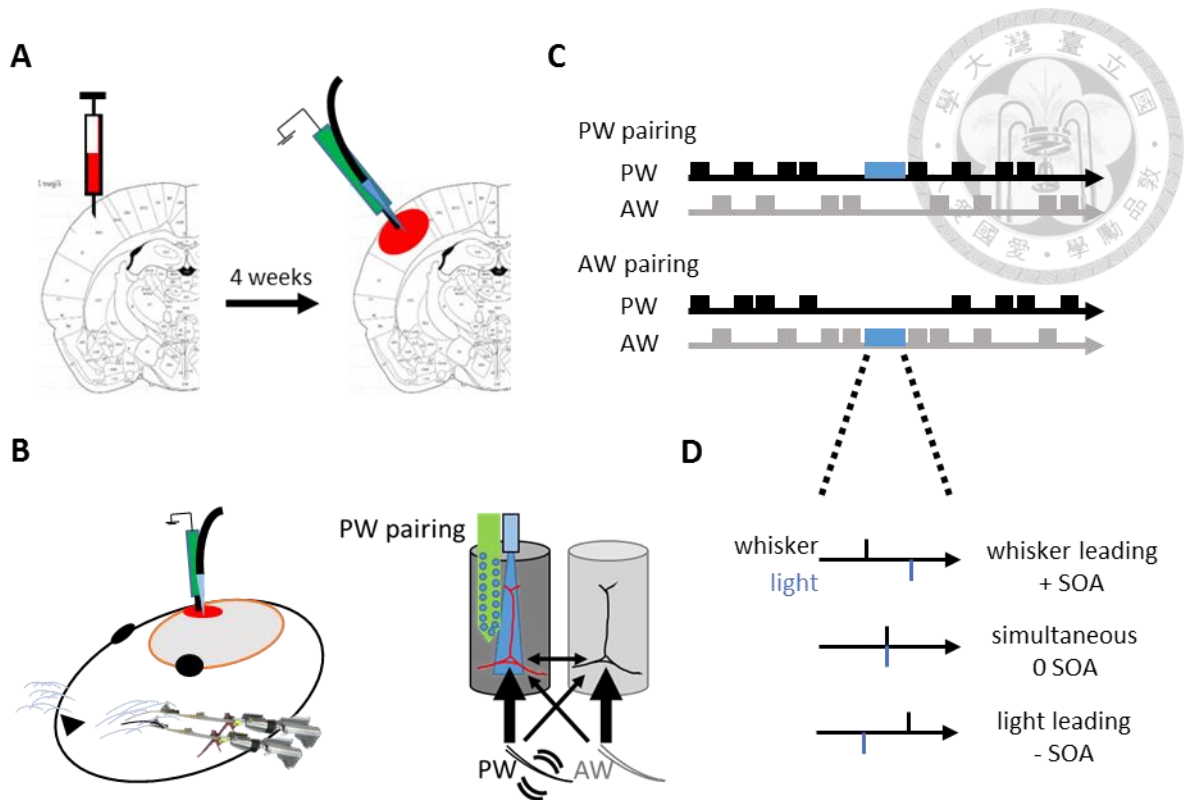
12

Figure 1. Experimental setups.
A. Adeno-associated virus targeting CaMKII expressing neurons is injected into the barrel field. After 4 weeks of infection, a recording electrode attached with a tapered optical stub is perpendicularly inserted into the ROI to perform extracellular electrophysiology while delivering light stimulus under program control. Red disc indicates infected area. **B.** Left: subject is anesthetized and head-fixed with two of its whiskers manually inserted into piezoelectric actuator based stimulators. Electrode is on the contralateral side of target whiskers. Right: A scheme of experimental design (a PW pairing example). **C.** There are four sessions of physical stimulus for PW and AW deflection before and after pairing session. The sequence of whisker stimulation is psedorandomly arranged. Only one whisker would be paired with light stimulus during pairing session. Thus, there are two conditions: PW pairing and AW pairing. **D.** In pairing session, there is various stimulus onset timing. The stimulus onset asynchrony (SOA) is defined as: (1) whisker leading (+ SOA), when whisker deflection starts earlier than light stimulus, (2) simultaneous (0 SOA), when two stimuli starts at the same time, and (3) light leading (- SOA), when light stimulus starts earlier than whisker deflection.
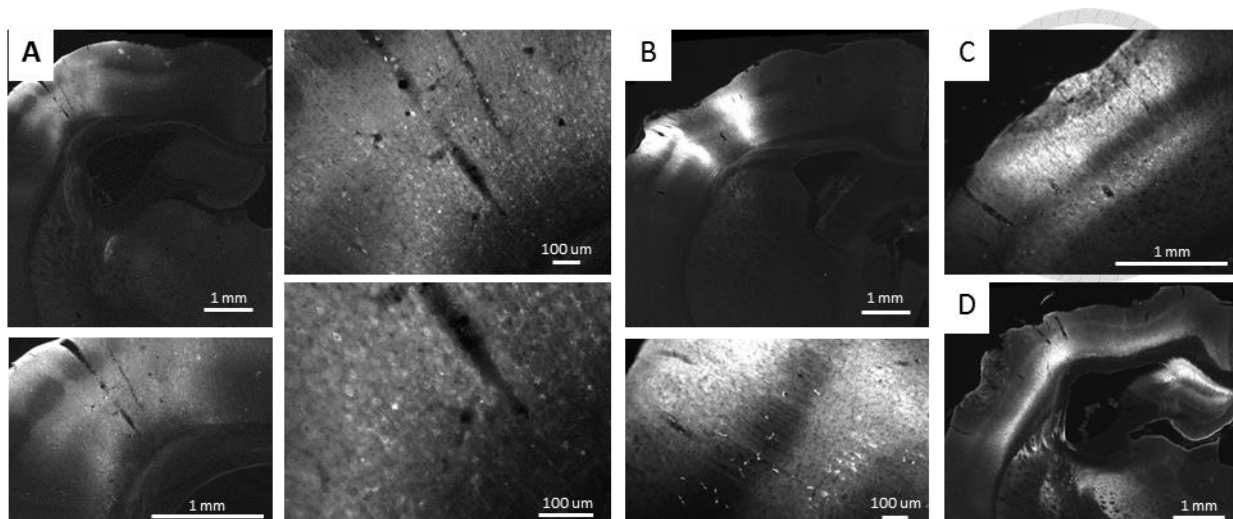
Figure 2. Histology of four different subjects under fluorescent microscope.
A. Left top: coronal section of 1/4 of an infected brain. Left bottom: magnified picture of infected area with tracts left by recording probe and optical fiber. Right: magnified pictures nearby the recording site. **B.** Top: coronal section of 1/4 brain. Bottom: Magnified picture of figure 2B top. **C.** Magnified picture. **D.** Coronal section of 1/4 brain. Fluorescent protein, mCherry, is shown in white.
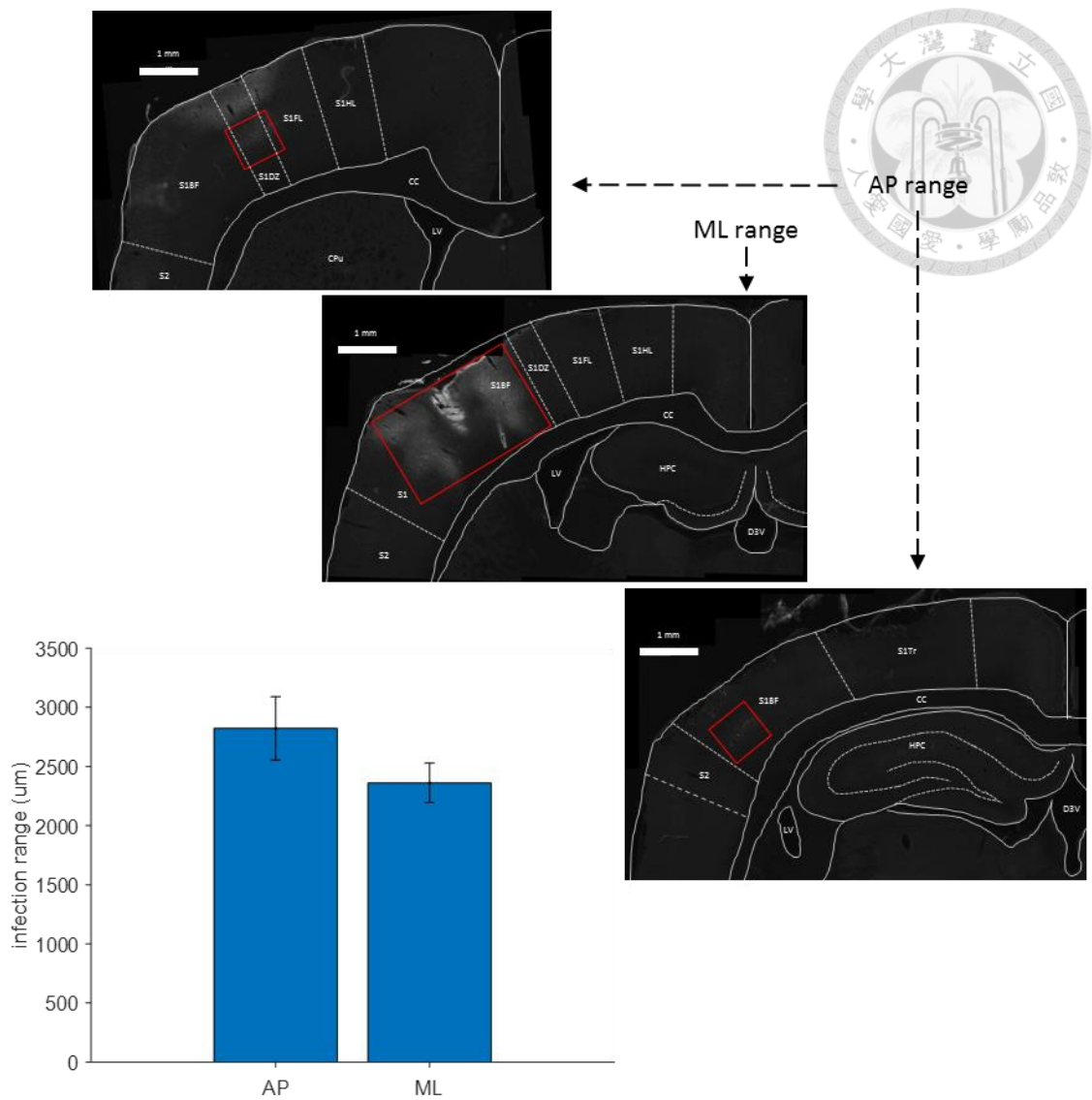
Figure 3. Estimation of infection range.

Infection range is defined in anterior-posterior (AP) and medial-lateral (ML) axes. AP range is defined as distance between anterior posterior end slices contained visible mCherry expressing cell body. ML range is defined as longest distance of visible mCherry expressing cell body tangentially along the neocortex at injection site (if found) or in the midst of AP range.

3. Results

3.1. Properties of Cell Samples

A single shank electrode (type E16, Cambridge NeuroTech) attached with an optical fiber was used to record single-unit signals in rat barrel cortex. From a total of 38 recording sessions in 17 rats, we included a total of 430 single units based on a 5-point spike-sorting system (see Methods for details). Two different types of stimulation were applied in the study: physical stimulation by deflecting a single whisker, and optical stimulation by briefly turning on a light source. All of the units were thought to be excitatory neurons because they expressed both CaMKII and channelrhodopsin and could be activated by optical stimulation (see Methods for details). The main goal of the study was to test whether neuronal responses induced by whisker deflection could be modulated by pairing physical stimulation with optical stimulation. Here we only included units that showed significant responses to both physical stimulation (for more than one whisker) and optical stimulation for further analysis ($n = 168$ out of 430, 39%). Figure 4A-B represents a cell example that responds to multiple whiskers and its spike waveform. Figure 4C shows that the example cell is a well-isolated single unit.

3.1.1. Responses evoked by physical stimulation.
Rat barrel field consisted of barrel columns which are topographically correspondent to mystacial pad whiskers (Petersen, 2007; Woolsey & Van der Loos, 1970). A neuron within a barrel column receives primary input from its corresponding whisker (defined as 'principal whisker') and some input from surround whiskers (Le Cam et al., 2011; Petersen, 2007; Simons, 1978; Wright & Fox, 2010). Here we defined a whisker as 'principal' or 'adjacent' based on neuronal responses induced by physical stimulation of a single whisker. The trajectory of whisker deflection was a combination of asymmetric sine waves with a 9-ms forward and

16

a 41-ms backward in one specific direction. The whisker was defected in the 8 possible directions separated from each other by 45 degrees (Fig. 4A, bottom).

The whisker triggered the largest evoked response was defined as a cell's principal whisker (PW), and the surrounding whisker that produced the second largest evoked response was defined as a cell's adjacent whisker (AW) in following paragraphs. Figure 4D represents the peristimulus time histograms (PSTH) of the whisker stimulation for an example cell. PW responses are shown at the left and AW responses at the right, and the response summations across 8 different directions are shown at the top. Onset latency was defined as the first bin after stimulus onset greater than 3 times of standard deviation of the baseline response in PSTH. The mean firing rate within 50 ms after onset latency was defined as the evoked response, and the mean firing rate within 50 ms before stimulus onset was defined as the baseline. The response induced by physical stimulation was considered significant if the evoked response was significantly greater than the baseline response in Wilcoxon rank sum test.

We found that the response generated by deflecting the PW was significantly faster and greater than the response generated by deflecting the AW (Fig. 5). Both the onset latency and the peak latency were shorter for PW responses than for AW responses (onset latency: PW: 11.29 ± 0.30 ms, AW: 12.80 ± 0.30 ms, $p < .001$; peak latency: PW: 19.84 ± 0.57 ms, AW: 24.53 ± 0.75 ms, $p < .001$; signed rank test). Furthermore, both the firing rate and the firing probability were significantly larger for PW responses than for AW responses (firing rate: PW: 7.05 ± 0.48 Hz, AW: 4.09 ± 0.37 Hz, $p < .001$; firing probability: PW: 0.41 ± 0.02, AW: 0.32 ± 0.02, $p < .001$; signed rank test). Expected number of action potential per trial within 50 ms after onset latency was defined as the firing rate. Greatest probability of any spike activity after stimulus onset in the 8 deflecting directions was defined as firing probability. Both PW and AW responses were significantly higher than

spontaneous activity (firing rate: 1.62 ± 0.17 Hz). The firing probability in our study was comparable to that in previous studies (de Kock et al., 2007; Petersen et al., 2003)
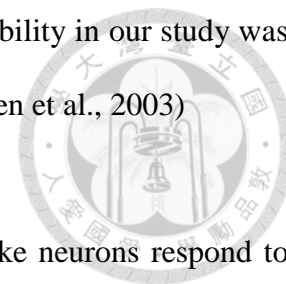
3.1.2. Responses evoked by optical stimulation. To make neurons respond to light, we microinjected the viral vector targeting CaMKII into rat barrel field about a month before the *in vivo* electrophysiological experiment. Success of the virus infection was confirmed by post-hoc histology of fluorescent microscopy observation and by the excitability of optical stimulation during electrophysiological recordings. We recorded neuronal activities evoked by optical stimulation (blue light, 473 nm in wavelength) at the surrounding of the injection site (usually 0.5-1 mm away). The density of infected neurons near the center of the injection site was too high to record well-isolated single units. Also, neurons at the center of the injection site might be injured by surgeries and became unresponsive to optical stimulation.

Figure 6A shows the response of an example cell induced by optical stimulation. Once the light was turned on, photo-evoked artifact was found at the beginning and the end of the optical stimulation for some neurons. The photo-evoked artifact was excluded from the estimation of response latency and firing rate. We found that the firing rate was modulated by the duration of optical stimulation (10-100 ms) but not the light intensity (2-10 mW) applied in the study (Fig. 6C; duration: $F(3,19) = 12.14$, $p < .001$; intensity: $F(2,19) = 1.21$, $p = .30$; interaction: $F(6,19) = 0.16$, $p = .99$; Two-way ANOVA, $n = 19$). Moreover, the firing probability evoked by optical stimulation was also influenced by the duration of light stimulation (Fig. 6D; duration: $F(3,19) = 96.94$, $p < .001$; intensity: $F(2,19) = 2.06$, $p = .13$; interaction: $F(6,19) = 0.24$, $p = .96$; Two-way ANOVA, $n = 19$). Based on these preliminary results, we thus used the following parameters for optical stimulation: strength of the optical stimulation: 5 mW or 10 mW, duration of the optical stimulation: 50 ms. The

firing probability reached a plateau (~70%) with a 50-ms duration (Fig. 6D).

We found that the onset latency was not different between physical stimulation and optical stimulation. On the other hand, the peak latency was significantly shorter for optical stimulation than for physical stimulation induced by PW (Fig. 7, onset latency: optical: 14.38 ± 1.89 ms, physical: 11.29 ± 0.30 ms, $p = .38$; peak latency: optical: 23.50 ± 2.03 ms, physical: 19.84 ± 0.57 ms, $p = .04$; Wilcoxon rank sum test). Moreover, both the firing rate and the firing probability were also significantly larger for optical stimulation than for physical stimulation induced by PW (Fig. 7, firing rate: optical: 39.29 ± 8.78 Hz, physical: 7.05 ± 0.48 Hz, $p < .001$; firing probability: optical: 0.794 ± 0.057, physical: 0.410 ± 0.015, $p < .001$; Wilcoxon rank sum test). These results indicated that optical stimulation could generate larger and more reliable responses than physical stimulation, and the physical-optical pairings might be suitable to induce neuroplasticity according to the spike timing dependent plasticity (STDP) paradigm (Jacob et al., 2007; Meliza & Dan, 2006).

3.2. Physical-Optical Pairing Experiment

Based on previous results of spike timing dependent plasticity (STDP) (Jacob et al., 2007; Meliza & Dan, 2006), repetitive sequenced activity of presynaptic and postsynaptic neurons would lead to changes in synaptic weighting. Here we tested whether the STDP paradigm could be applied *in vivo* in the barrel cortex, in which optical stimulation affected a large number of neurons and a complex neuronal circuitry.

We hypothesized that neuronal properties, including response latency, firing rate and probability, and direction selectivity, might change after repetitive pairings of the physical stimulation and the optical stimulation. Furthermore, we wanted to test whether the potential neuroplasticity induced within the principal whisker (PW) or the adjacent whisker (AW) could affect properties of neighboring whiskers. We also hypothesized that the
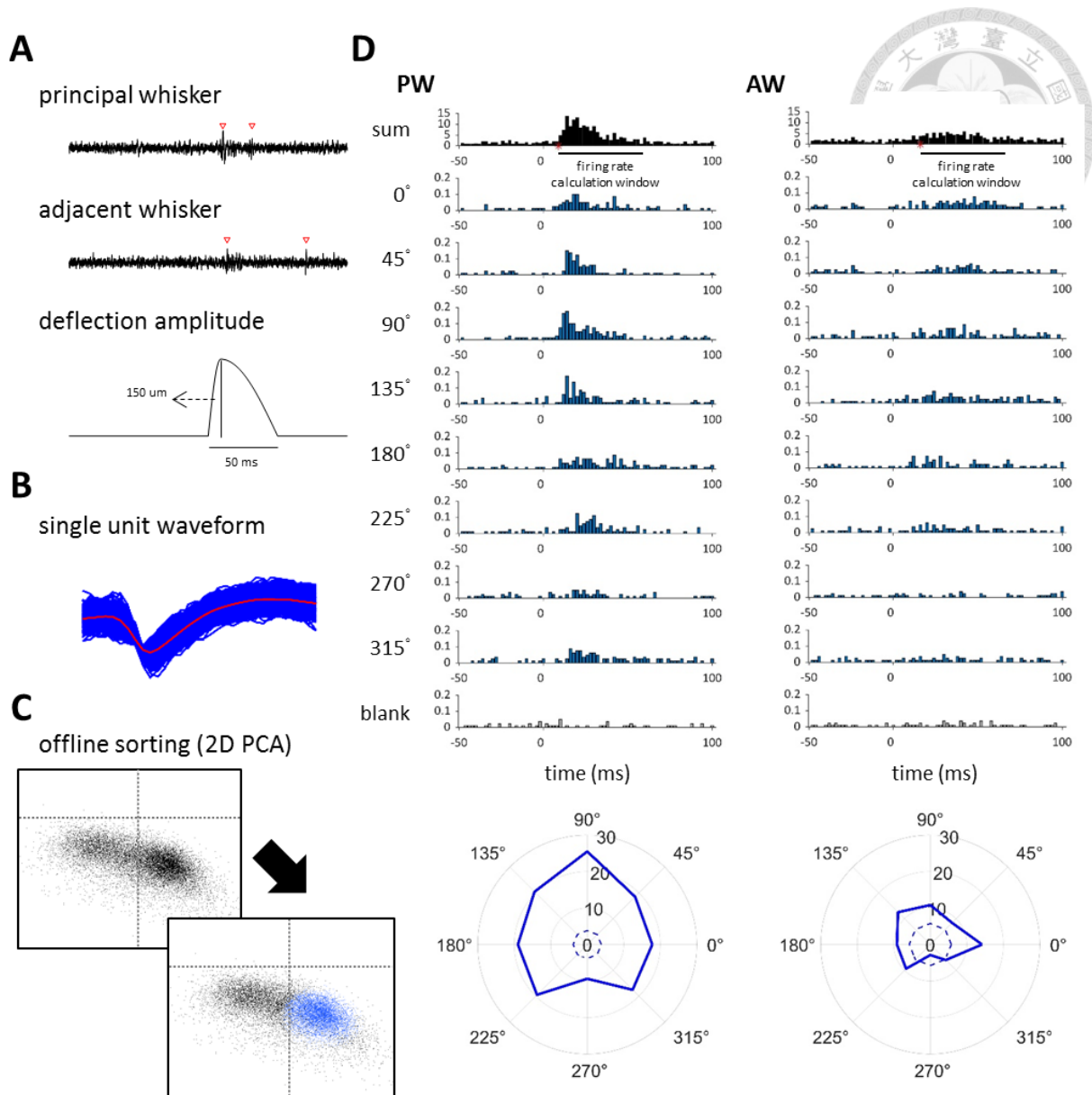
Figure 4. Extracellular single unit recording of physical stimulus evoked activity.
A. High pass filtered extracellular recorded signals (250 Hz threshold). Principal whisker
and adjacent whisker are deflected separately in time, both stimulus could drive single
unit activity. Whisker stimulation is composited of asymmetric sinusoid wave, with a
steep rise period of 9 ms and a slow fall period of 41 ms. **B.** Example unit's spike
waveform. **C.** Offline sorting is performed to isolate single unit activity. Top left: signals
passed spike detection threshold are distributed in 2D PCA panel based on their spike
waveform. Bottom right: the clustered blue dots are determined as a single unit. Black
dots are signals considered as noise or signals from other units. **D.** PSTH of whisker
stimulation. Black bars indicate response summations across all deflection directions.
Blue bars indicate PSTH in one deflection direction. Bottom, polar plots show angular
preference of the example unit. Evoked firing rate is defined as averaged number of
action potentials within 50 ms after response onset. Spontaneous firing rate is defined as
averaged number of action potentials within 50 ms before stimulus onset. Solid lines
represent evoked firing rates. Dashed lines represent spontaneous firing rates.

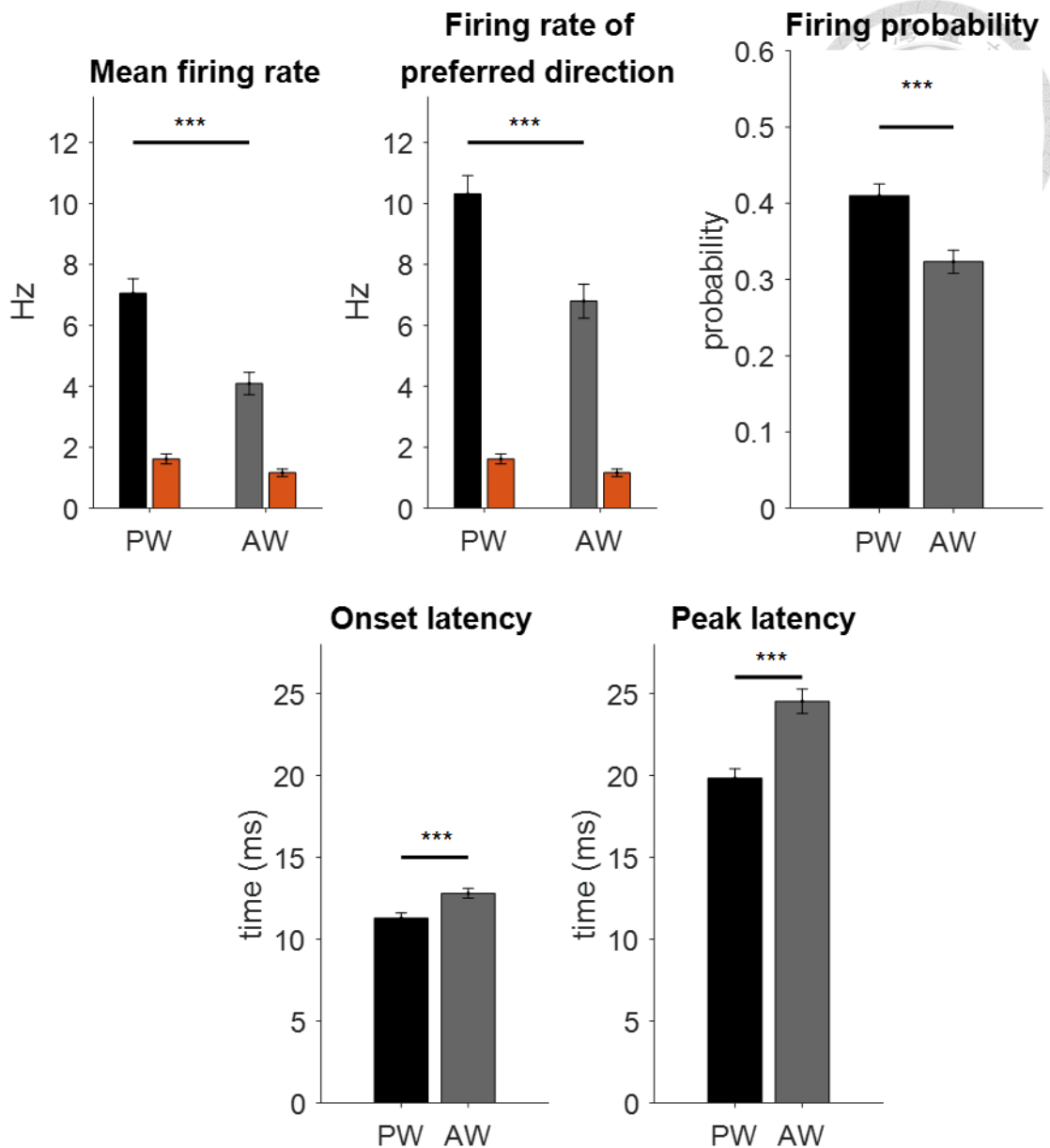*Figure 5.* Difference between PW and AW deflection evoked response.
Top left: Mean firing rate of all deflection direction. Bottom middle: firing rate of deflection in preferred direction. Black bars indicate PW deflection evoked firing rate, gray bars indicate evoked firing rate, and orange bars indicate spontaneous firing rate. Top right: probability of evoking neuronal activity. Bottom: onset latency and peak latency.
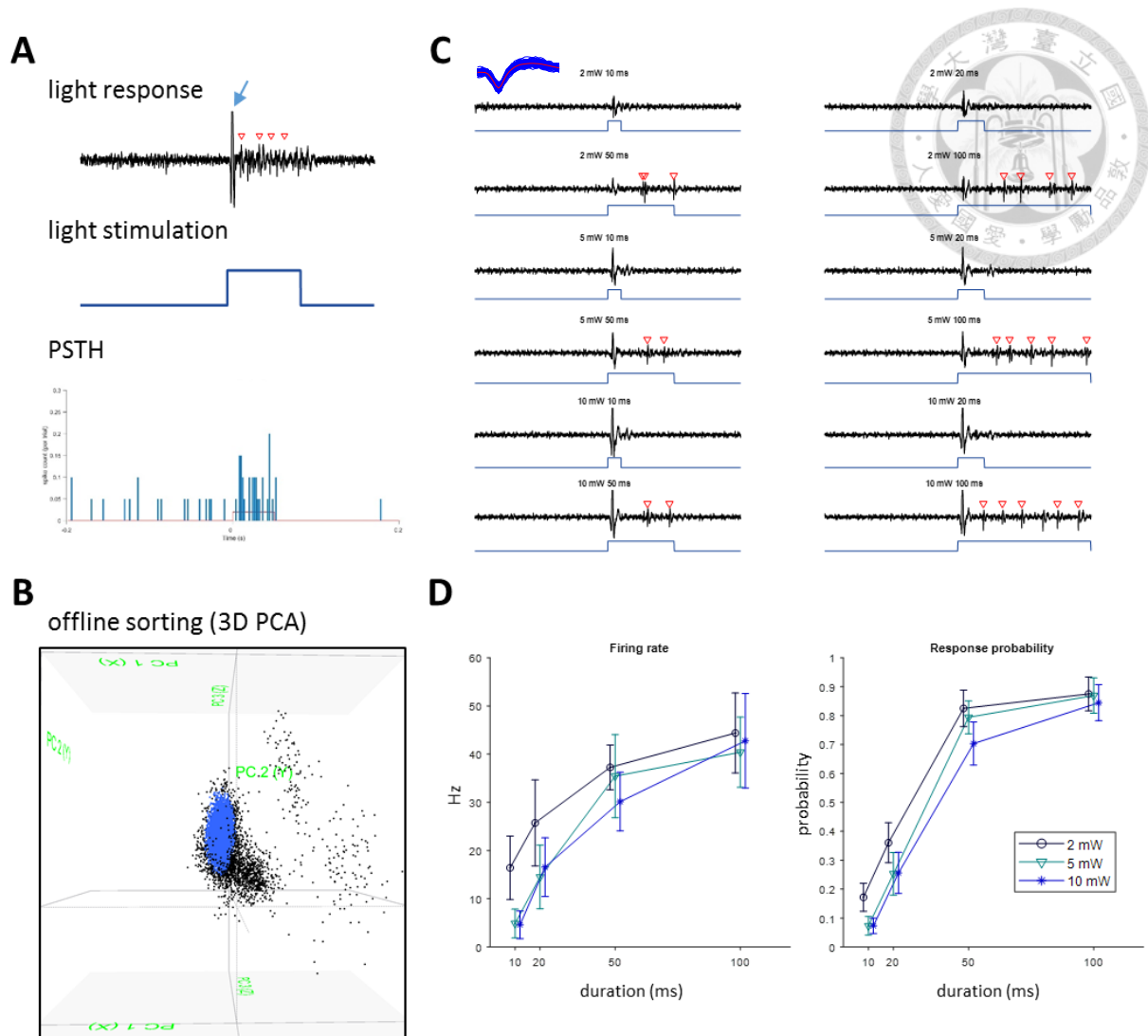
Figure 6. Extracellular single unit recording of light stimulus evoked optogenetic activity.
A. High pass filtered extracellular recorded signals (250 Hz threshold). Light stimulus of 50 ms duration is delivered to the somatosensory cortex through optical fiber. Red triangles indicate timing of action potential of the sorted single unit. Blue arrow indicates light stimulation evoked compound response. Bottom, PSTH of light stimulation. Blue lines indicate neuronal activity. Red square indicates period of light stimulation. **B.** Offline sorting is performed to isolate single unit activity. Signals passed spike detection threshold are distributed in 3D PCA panel based on their spike waveform. The clustered blue dots are determined as the example unit. Black dots are signals considered as noise or signals from other units **C.** High pass filtered signals for another example unit's light evoked activity under different parameters. **D.** Light evoked response in different intensity and duration ($N = 17$). Firing rate is defined as averaged number of action potentials trough out entire duration of light stimulation. Firing probability is the ratio of responsive trials to total trials.

Figure 7. Difference between physical (PW) and light stimulation evoked response. Top: onset latency and peak latency. Bottom left: mean firing rate. Black bars indicate physical stimulus (PW) evoked firing rate, blue bars indicate evoked firing rate, and orange bars indicate spontaneous firing rate. Bottom right: probability of evoking neuronal activity.
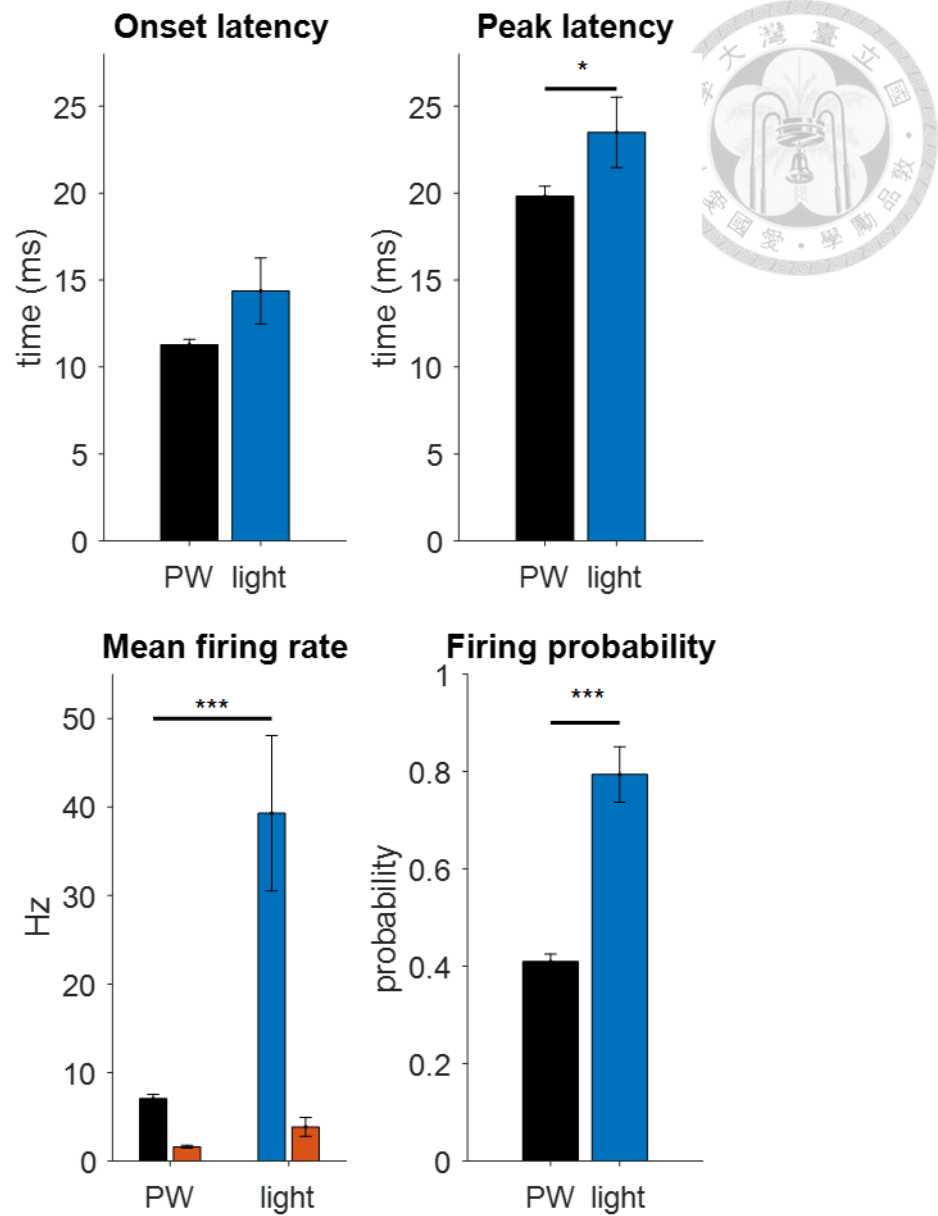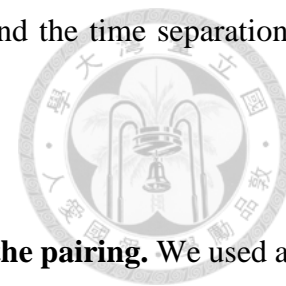
degree of the STDP-induced change might depend on the order and the time separation between the two stimuli.

3.2.1. Changes in response properties before and after the pairing. We used a randomized block design to detect the change before and after the physical-optical pairing. The block design consisted of 4 whisker-only blocks, followed by 5 whisker-optical pairing blocks, and followed by another 4 whisker-only blocks. Within a whisker-only block, only one whisker (either PW or AW) was deflected at a time and was defected randomly in one of the 8 different directions. Each direction was repeated 20 repeats, so there was a total of 160 trials in one whisker-only block. For each trial in the whisker-only block, the stimulation was on for 50 ms followed by a 75 ms inter-stimulus interval. Within a whisker-optical pairing block, the selected whisker (either PW or AW) was deflected 20 times only in one direction (usually the preferred direction of the cell), and the stimulus onset asynchrony (SOA) between the whisker stimulation and the optical stimulation was fixed (a total of 100 repeats in 5 pairing blocks). Each pairing trial was conducted in 1Hz frequency: the paired stimuli lasted for 50~90 ms (different SOAs), followed by an inter-stimulus interval of 910~950 ms. We monitored changes in evoked responses for both PW and AW.

Figure 8 represents the response (raster plots, averaged PSTHs, polar plots) of a cell example before and after the physical-optical pairing. In the example cell, PW is the selected whisker for pairing. In this example, we found that the PW-pairing had no effect on PW responses but had a strong effect on AW responses – the firing rate of AW (based on mean responses across the 8 different directions) was significantly lower after the pairing. Overall, ~49% of the cell population ($n = 82/168$) showed significant changes in the mean firing rate across all deflection directions after the physical-optical pairing (Fig.

24

9A; 43% ($n = 41/95$) in the PW-pairing condition and 56% ($n = 41/73$) in the AW-pairing condition). We then divided the data into four different conditions: the change in PW and AW response after the PW-pairing, and the change in PW and AW responses after the AW-pairing.
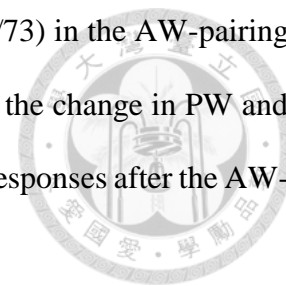
Overall, we found that, among the cells in PW-pairing condition, 22% showed changes only in PW responses ($n = 21/95$), and 9% showed changes only in AW responses ($n = 9/95$), and 12% showed changes both in PW and AW responses ($n = 11/95$). On the other hand, among the cells in AW-pairing condition, 22% showed changes only in PW responses ($n = 16/73$), and 23% showed changes only in AW responses ($n = 17/73$), and 11% showed changes both in PW and AW responses ($n = 8/73$) (Fig. 9B).

These results indicated that the whisker-optical pairing has a strong effect on the mean firing rate, suggesting that the neuroplasticity could be induced *in vivo* in the barrel cortex. The modulation effect seemed to be greater in PW-deflected activities than in AW-deflected activities.

Besides the firing rate, the physical-optical pairing did not alter the onset latency, the peak latency, and the firing probability of PW and AW responses (see Table 1, all comparisons were based on signed rank test). Table 1 shows the means and stand deviations for the four different conditions: PW-change under PW-pairing, AW change under PW pairing, PW change under AW-pairing, and AW change under AW-pairing. Data under different SOA conditions were first combined in the analyses (we addressed the SOA effect in a latter section). At population level, the onset latency and the peak latency were not changed after the whisker-optical pairing (data are shown in the following order: PW response under PW-pairing, AW response under PW pairing, PW response under AW-pairing, and AW response under AW-pairing, respectively). Onset latency was 11.18 ± 0.43, 12.14 ± 0.41, 11.43 ± 0.43, 13.65 ± 0.43 ms before pairing and 11.35 ± 0.44, 12.70 ±

0.40, 11.39 ± 0.42, 14.11 ± 0.40 ms after pairing, in the same order with Table 1. No significant difference was observed in any condition using signed rank test. Peak latency was 20.24 ± 0.81, 24.72 ± 1.10, 19.30 ± 0.78, 24.28 ± 0.96 ms before pairing and 20.14 ± 0.84, 25.39 ± 1.33, 19.83 ± 0.88, 26.09 ± 1.20 ms after pairing, in the same order with Table 1. No significant difference was observed in any condition using signed rank test.

Firing probability was also not changed after pairings (data are shown in the following order: PW response under PW-pairing, AW response under PW pairing, PW response under AW-pairing, and AW response under AW-pairing, respectively). Firing probability was 0.43 ± 0.02, 0.31 ± 0.02, 0.39 ± 0.02, 0.35 ± 0.02 before pairing and 0.43 ± 0.02, 0.31 ± 0.02, 0.39 ± 0.02, 0.35 ± 0.02 after pairing, in the same order with Table 1. No significant difference was observed in any condition using signed rank test.

If we focused on units with changed mean firing rate, firing probability of these units slightly decreased only in AW responses under PW-pairing (Before: 0.44 ± 0.04; after: 0.39 ± 0.04; $p = .026$, signed rank test). Firing rate was adjusted with subtraction of baseline activity in order to eliminate individual differences. Adjusted firing rate was not changed after pairings (data are shown in the following order: PW response under PW-pairing, AW response under PW pairing, PW response under AW-pairing, and AW response under AW-pairing, respectively). Adjusted firing rate was 5.69 ± 0.56, 2.76 ± 0.34, 5.11 ± 0.58, 3.14 ± 0.50 Hz before pairing and 5.85 ± 0.57, 2.54 ± 0.30, 4.86 ± 0.48, 2.97 ± 0.40 Hz after pairing, in the same order with Table 1. No significant difference was observed in any condition using signed rank test.

3.2.2. Firing probability.

We found that almost half of our cell samples showed significant changes in firing rate between before and after the whisker-optical pairing, and among them both upregulation and downregulation were observed. What factor might

26

contribute to the directional different in neuroplasticity? Here we compared the changes in the mean firing rate with the firing probability for each neuron. We hypothesized that neurons with higher firing probabilities would show higher degree of neuroplasticity because the strong feedforward input might be influenced more strongly by the whisker-optical pairing. In contrast, neurons with lower firing probabilities would show lower degree of neuroplasticity because the feedforward input was relatively weak and therefore less affected by the whisker-optical pairing. Previous studies had shown that the rodent barrel cortex was characterized of low evoked responses by physical stimulation. The firing probability, rather than the mean firing rate, might be a better candidate to represent the strength of the feedforward input.

Figure 10 represents the comparisons between the firing rate change (before and after the whisker-optical pairing) and the firing probability (before the pairing) under four different conditions (from left to right): PW response under PW-pairing, AW response under PW pairing, PW response under AW-pairing, and AW response under AW-pairing. Overall, the mean firing rate was unchanged or increased slightly for neurons with low firing probability. In contrast, the amplitude of the firing rate change increased among cells with higher firing probability, and most cells were downregulated in the mean firing rate. We found that the firing rate change was negatively correlated with the original firing probability induced by whisker stimulation only in the AW-pairing condition (Fig. 10B right, PW evoked response: $r = -0.47$, $p < .001$; AW evoked response: $r = -0.48$, $p < .001$, Pearson correlation). However, this only shown in AW responses under PW-pairing condition (Fig. 10B left, PW evoked response: $r = -0.18$, $p = .09$; AW evoked response: $r = -0.23$, $p = .02$, Pearson correlation).

Similar results were also observed in firing rate of paired direction (Fig. 10C left, PW evoked response: $r = -0.14$, $p = .19$; AW evoked response: $r = -0.18$, $p = .08$, Pearson

correlation; Fig. 10C right, PW evoked response: r = -0.43, p < .001; AW evoked response: r = -0.34, p = .003, Pearson correlation). The only difference was there was no negative correlation in AW responses under PW-pairing.

These results indicated that the change of neuronal activity was related to original state of the neuron, though it was unclear why the effect of AW-pairing differed from that of PW-pairing. It was possible that the AW-pairing mostly affects the cortico-cortical network that was critical for surround suppression. Therefore, the decrease in the mean firing rate was likely due to the enhancement of the surround suppression.

3.2.3. Preferred direction. When conducting the whisker-optical pairing, one of the 8 directions was randomly selected to pair with the optical stimulation. We next investigated whether stimulus feature plays an important role in functional plasticity. Initially, we aligned directional tuning curves for the entire population to their preferred directions. A robust decrease of response in preferred direction after pairing was observed under all conditions (PW responses under PW-pairing, AW responses under PW-pairing, PW responses under AW-pairing and AW responses under AW-pairing). While the responses of rest directions showed variability.

In order to better explain the variability of directional response changes, paired directions were first divided into three different groups based on the difference between the neuron's preferred direction and the paired direction (see Fig. 11): preferred (the difference was equal to or smaller than 45 degree), orthogonal (the difference was equal to 90 degree) and non-preferred (the difference was equal to or larger than 135 degree).

We found that the difference between the neuron's original preferred direction and the paired direction has a strong effect on whether the neuron was upregulated or downregulated, especially in the PW-pairing condition (Fig. 11C). In the PW-pairing

28

condition, the mean response of PW was upregulated in the non-preferred condition (firing rate change index: 0.11 ± 0.06; $p = .006$, Wilcoxon rank sum test), resembling closely the effect of disinhibition. In contrast, the mean response of PW was downregulated in the preferred condition (firing rate change index: -0.08 ± 0.05; $p = .04$, Wilcoxon rank sum test), resembling closely the effect of adaptation. No significant change in the PW response in the orthogonal. We found that there was an interaction between experimental condition and paired direction for PW response in PW-pairing condition, indicating paired direction was an important factor in our manipulation.

On the other hand, difference was found neither in AW responses under PW-pairing condition, nor in AW or PW responses under AW-pairing condition. Therefore, the difference between the neuron's original preferred direction and the paired direction has a strong effect on PW responses only when PW deflection was paired. This effect was most likely involved only the feedforward network.

To capture a whole picture of neuronal activity change, we also calculated firing rate change of mean evoked response of all deflection directions. We found that there was no main effect for paired direction on mean firing rate change (Fig. 11C).

3.2.4. Different stimulus onset asynchrony in the pairing.

3.2.4. Different stimulus onset asynchrony in the pairing. Based on the STDP rules (Bi & Poo, 1998; Feldman, 2012), we also applied different conditions of stimulus onset asynchrony (SOA, between -40 ms to 40 ms between the whisker stimulation and the optical stimulation) to modulate the degree of neuroplasticity *in vivo* in the barrel cortex (Fig. 12A). The SOA was quantified as the peak latency induced by the optical stimulation subtracted from the peak latency induced by the whisker stimulation in the pairing condition. The SOA was positive if the whisker response peak was earlier than the optical response peak (whisker response leading), and was negative if the whisker response peak

was later than the optical response peak (optical response leading). Including these SOAs were also important for figuring out the suitability of optogenetic tools as a potential candidate for *in vivo* cell-type-targeting neuroplasticity guider. In order to compare population data, we calculated the normalized change ratio in firing rate (ranged between -1 and 1) before and after the whisker-optical pairing for the entire cell population.

To our surprise, we did not find similar response pattern in the STDP paradigm (bidirectional plasticity) under our SOA manipulations (Fig. 12C). In both whisker response leading and optical response leading conditions, both upregulation and downregulation in mean firing rate were found across all different SOAs. These results suggested that the STDP rules might not be applied in the in vivo condition, which involved a larger number of neurons and a more complex brain circuitry.

3.2.5.   Spontaneous firing rate. In order to verify whether the manipulation caused a global change of neuronal state, we compared spontaneous firing activities before and after pairings. Here we defined spontaneous firing as mean firing rate of 50-ms time window in blank trials in whisker stimulation sessions. We found that the optical-physical pairings did not cause significant changes in spontaneous firing activities (Fig. 13). Only 2.4% of units ($n = 4/168$) manifested changes in their baselines. Two units showed an increase in spontaneous firing rate (PW response ($n = 1$) and AW response ($n = 1$) under PW pairing), and two units showed a decrease in spontaneous firing rate (PW response ($n = 1$) and AW response ($n = 1$) under PW pairing).

3.2.6.   Direction selectivity. As we deflected paired whisker in one direction across entire pairing session, we would like to know whether direction selectivity of units changed according to the paired direction. We defined a preferred direction for each unit

based on the vector sum of evoked responses in 8 cardinal directions. Then the angular difference between the preferred direction and the paired direction was calculated before and after pairing, respectively. Reduction of angular difference could be considered as a traction of direction selectivity toward the paired direction, while increase of angular difference could be considered as a repulsion of direction selectivity from the paired direction.

There was no preferred direction change for population data under any of the four conditions (p = .112, .973, .923, and .088, signed rank test). We here simply defined a change greater than $45°$ as a criteria of preferred direction change for each single unit. We found preferred direction was not changed for most of the units: 64% in PW responses under PW-pairing (n = 61/95), 47% in AW responses under PW-pairing (n = 45/95), 55% in PW responses under AW-pairing (n = 40/73), and 56% in AW responses under AW-pairing (n = 41/73). Among units with changes in preferred directions after the parings (~40%), about half of them preferred the direction closer to the paired direction, whereas about half of them preferred the direction away from the paired direction: 18% and 18% in PW responses under PW-pairing (n = 17/95 & 17/95), 24% and 28% in AW responses under PW-pairing (n = 23/95 & 27/95), 21% and 25% in PW responses under AW-pairing (n = 15/73 & 18/73), and 26% and 18% in AW responses under AW-pairing (n = 19/73 & 13/73) (Fig. 14).

3.2.7. **Pairing success rate.** We estimated the trial number of successful inductions of both optical and physical response in optical-physical pairing in consideration of the low evoked rate to physical stimulation of the rodent barrel cortex. Accordingly, we could verify whether success rate played a role in the significance and magnitude of

31

neuronal response changes.

Previous studies using STDP protocol reported various sufficient numbers of trials to guide neuroplasticity. In most *in vitro* studies, the success rate of pairings was faithfully high because of the usage of direct current injections to the presynaptic area or the patched neurons. On the other hand, *in vivo* studies might suffer from jitter or variation of spike timing in pairings caused by the intact connection in the brain and therefore could be unable to induce postsynaptic activities. We here defined success rate in pairings as the percentage of trials in which both optical evoked response and physical evoked response were detectable in each trial. The detection time window was defined as the 30-ms width that covered the two response peaks induced by physical and optical stimulations (see Fig. 15A).

Figure 15B shows that the pairing success rate was not a congruent indicator of neural activity changes. Only in PW-pairings, we found magnitude of firing rate change positively correlated with success rate (except for firing rate of the paired direction in AW responses). On the other hand, firing rate change index did not correlate with the success rate (only except for AW responses under PW-pairings, a negative correlation). It is possible that a minimum trial number was sufficient to induce neuronal activity change or our estimation of success rate failed to represent pairing details such as subthreshold activities.

3.2.8. **Regression.** We applied a stepwise multiple linear regression for a further investigation of to what degree could we explain neuronal activity changes with abovementioned factors. Neural activity changes were introduced as dependent variable (response) one at a time. Thus, there were totally eight regression models (firing rate change & firing rate change index for: mean firing rate, firing rate of paired direction, firing rate of preferred direction, and spontaneous firing rate). Tested whisker identity (PW or AW), pairing condition (PW pairing or AW pairing), SOA, firing probability before pairing,

paired direction and interaction term between each factor were introduced as independent variables (predictors) to a stepwise multiple linear regression model in MATLAB regression learner APP. A final model for survived factors was generated by the APP, which also returned regression model, adjusted R-squared and coefficients.

In Table 2, we found low adjusted R-squared, less than 0.2, for all dependent variables, which indicated we could not well predict neuronal activity changes based on the currently used factors. Details such as independent variables (predictors), coefficients and p-values for abovementioned models were listed in Table 3.
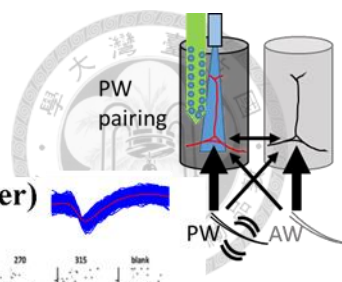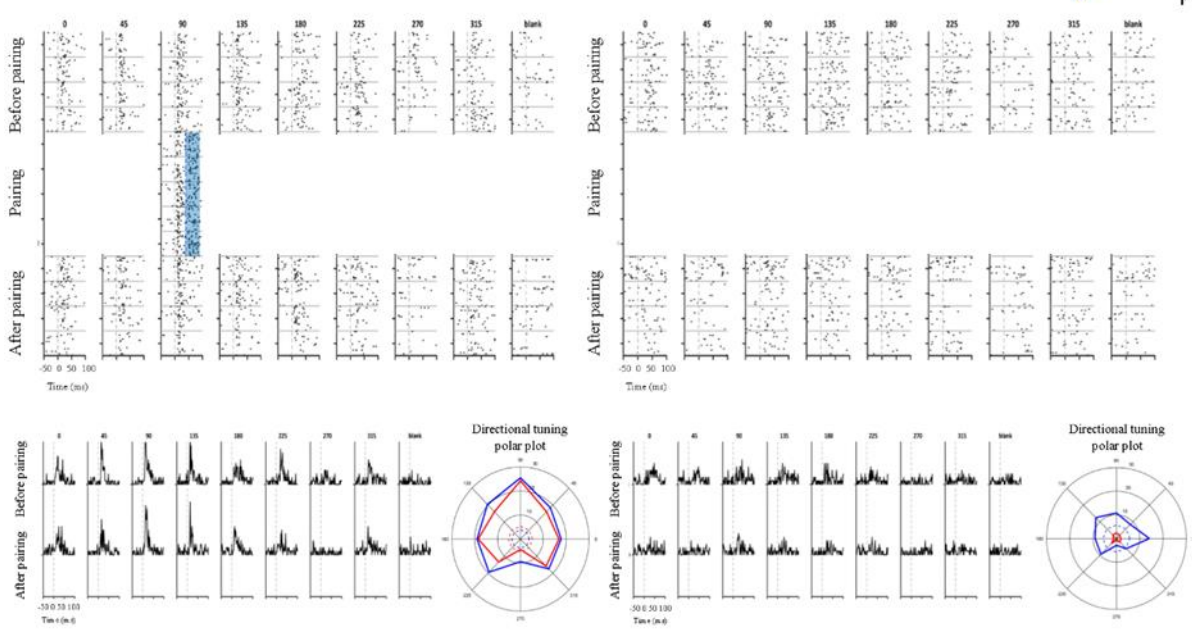
Figure 8. Neuronal activity throughout pairing experiment (a PW pairing example). Raster plot and averaged PSTH of each deflection direction of physical stimulus. Polar plot is used to summarize direction selectivity of the example unit. Top right, scheme of PW pairing. An extracellular electrode attached with a fiber stub was inserted into a barrel column. In the duration of physical-optical pairing, blue light stimulation and PW deflection would be delivered to recorded neurons. Width of arrow indicates different weighting of PW and AW pathway connected to the recorded barrel column. Waveform of this example unit is plot in blue with an averaged waveform plot in red.
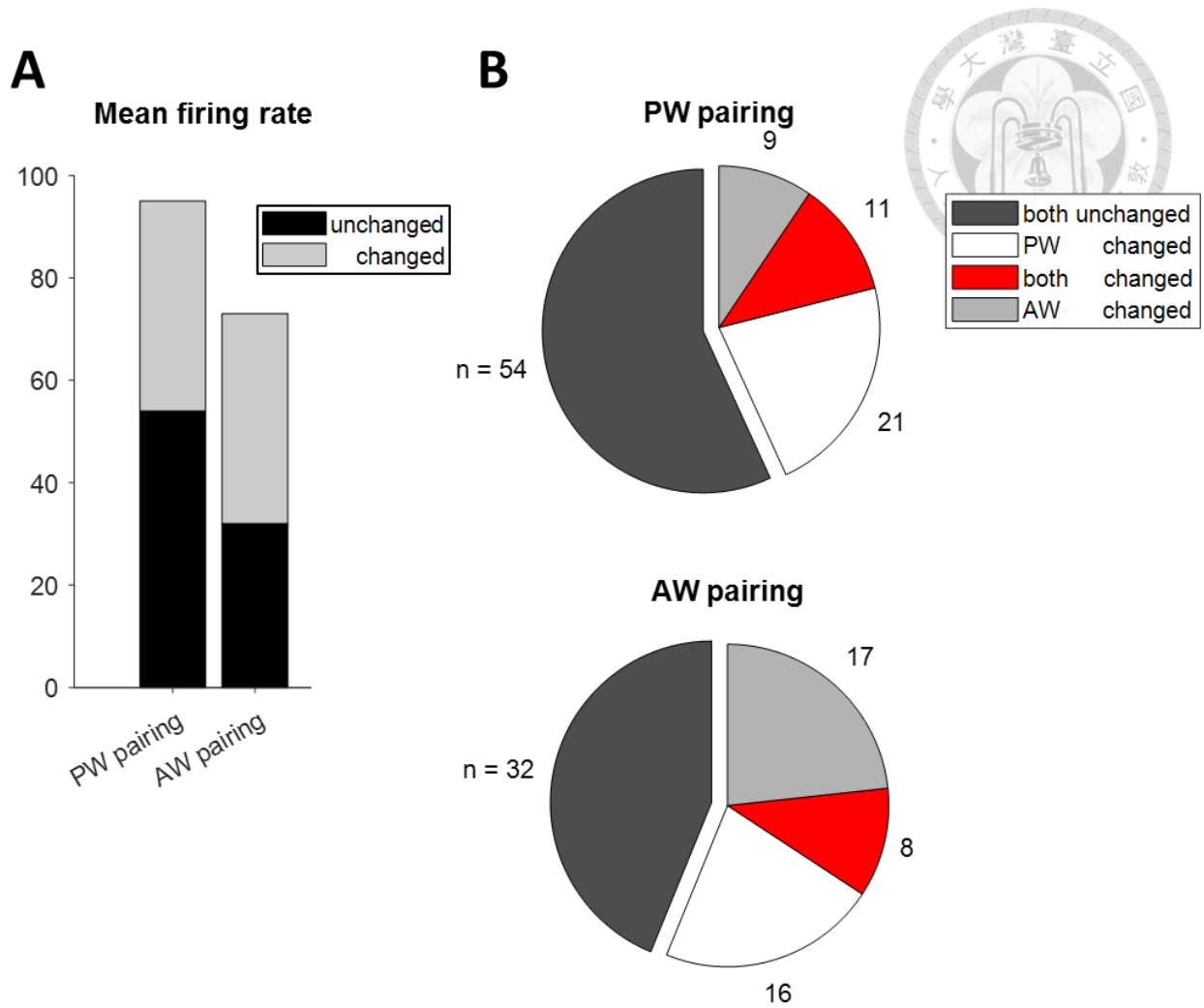
34

Figure 9. Number of recorded units.
A. We include 168 single units showed significant evoked response to PW, AW and optical stimulation. There are 95 units in PW pairing group and 73 units in AW pairing group. The bar chart shows about half of units' responses to physical stimulation changed after physical-optical pairing. **B.** Summary of physical stimulus evoked activity change.

Table 1

Population Data of Different Response Properties Before and After the Pairing

		PW pairing		AW pairing	
		PW	AW	PW	AW
N number	all	95	95	73	73
	[mean]	[32]	[20]	[24]	[25]
	(pd)	(6)	(3)	(4)	(0)
onset latency (ms)	before	11.18 ± 0.43	12.14 ± 0.41	11.43 ± 0.43	13.65 ± 0.43
		[12.53 ± 0.72]	[13.03 ± 0.88]	[11.97 ± 0.87]	[12.77 ± 0.78]
		(10.83 ± 1.72)	(14.33 ± 2.89)	(13.63 ± 2.56)	(N/A)
	after	11.35 ± 0.44	12.70 ± 0.40	11.39 ± 0.42	14.11 ± 0.40
		[12.16 ± 0.74]	[13.07 ± 0.97]	[11.59 ± 0.71]	[13.98 ± 0.66]
		(11.33 ± 1.55)	(14.78 ± 3.42)	(13.21 ± 1.64)	(N/A)
peak latency (ms)	before	20.24 ± 0.81	24.72 ± 1.10	19.30 ± 0.78	24.28 ± 0.96
		[22.48 ± 1.59]	[24.20 ± 1.74]	[21.08 ± 1.46]	[25.13 ± 1.77]
		(19.92 ± 3.70)	(22.17 ± 1.01)	(26.75 ± 4.70)	(N/A)
	after	20.14 ± 0.84	25.39 ± 1.33	19.83 ± 0.88	26.09 ± 1.20
		[21.99 ± 1.70]	[22.93 ± 1.11]	[20.36 ± 1.13]	[25.33 ± 2.05]
		(18.50 ± 2.65)	(23.89 ± 2.16)	(25.58 ± 4.17)	(N/A)
firing rate (Hz)	before	5.69 ± 0.56	2.76 ± 0.34	5.11 ± 0.58	3.14 ± 0.50
		[5.36 ± 0.91]	[4.64 ± 1.13]	[5.54 ± 1.05]	[2.45 ± 0.49]
		(17.87 ± 3.36)	(5.85 ± 0.98)	(8.29 ± 4.06)	(N/A)
	after	5.85 ± 0.57	2.54 ± 0.30	4.86 ± 0.48	2.97 ± 0.40
		[5.59 ± 0.90]	[3.87 ± 0.93]	[4.90 ± 0.70]	[2.77 ± 0.42]
		(17.19 ± 5.45)	(6.73 ± 4.70)	(6.19 ± 1.96)	(N/A)
firing probability	before	0.429 ± 0.020	0.306 ± 0.020	0.385 ± 0.022	0.345 ± 0.023
		[0.45 ± 0.03]	[0.44 ± 0.04]	[0.43 ± 0.04]	[0.35 ± 0.03]
		(0.71 ± 0.09)	(0.38 ± 0.06)	(0.44 ± 0.14)	(N/A)
	after	0.433 ± 0.020	0.314 ± 0.018	0.387 ± 0.019	0.346 ± 0.019
		[0.45 ± 0.03]	[0.39 ± 0.04]	[0.41 ± 0.03]	[0.36 ± 0.03]
		(0.67 ± 0.11)	(0.43 ± 0.17)	(0.37 ± 0.10)	(N/A)

Note. Data were separated into four different conditions (from left to right): PW response under PW-pairing, AW response under PW pairing, AW response under AW-pairing, and PW response under AW-pairing. Within each cell, the top row represents data for the all cells, the second row represents data for those cells showing significant changes in the average across all directions before and after the pairing (abbreviated as [mean]), and the third row represents data for those cells showing significant changes only in the paired direction before and after the pairing (abbreviated as (pd)).
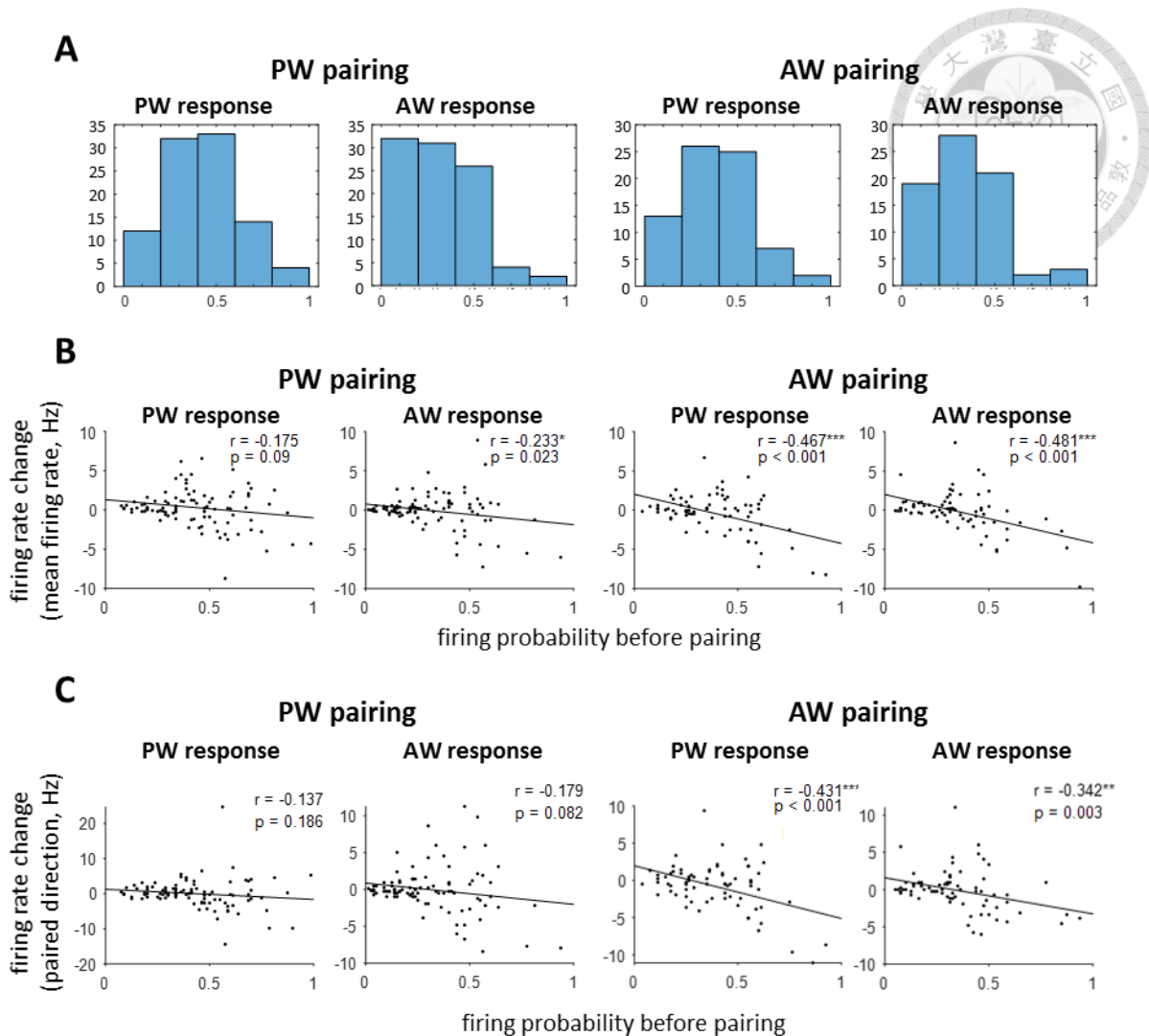
Figure 10. Relationship between firing rate change and firing probability before pairing.
A. Histograms of firing probability before pairing for PW and AW in PW pairing and
AW pairing condition. **B.** Correlation between firing probability before pairing and mean
firing rate change. Negative slopes are observed in both PW and AW evoked response
under both pairing conditions. Both PW and AW evoked firing rate changes are
negatively correlated with recorded neurons' original firing probability under AW pairing
condition. **C.** Correlation between firing probability before pairing and firing rate change
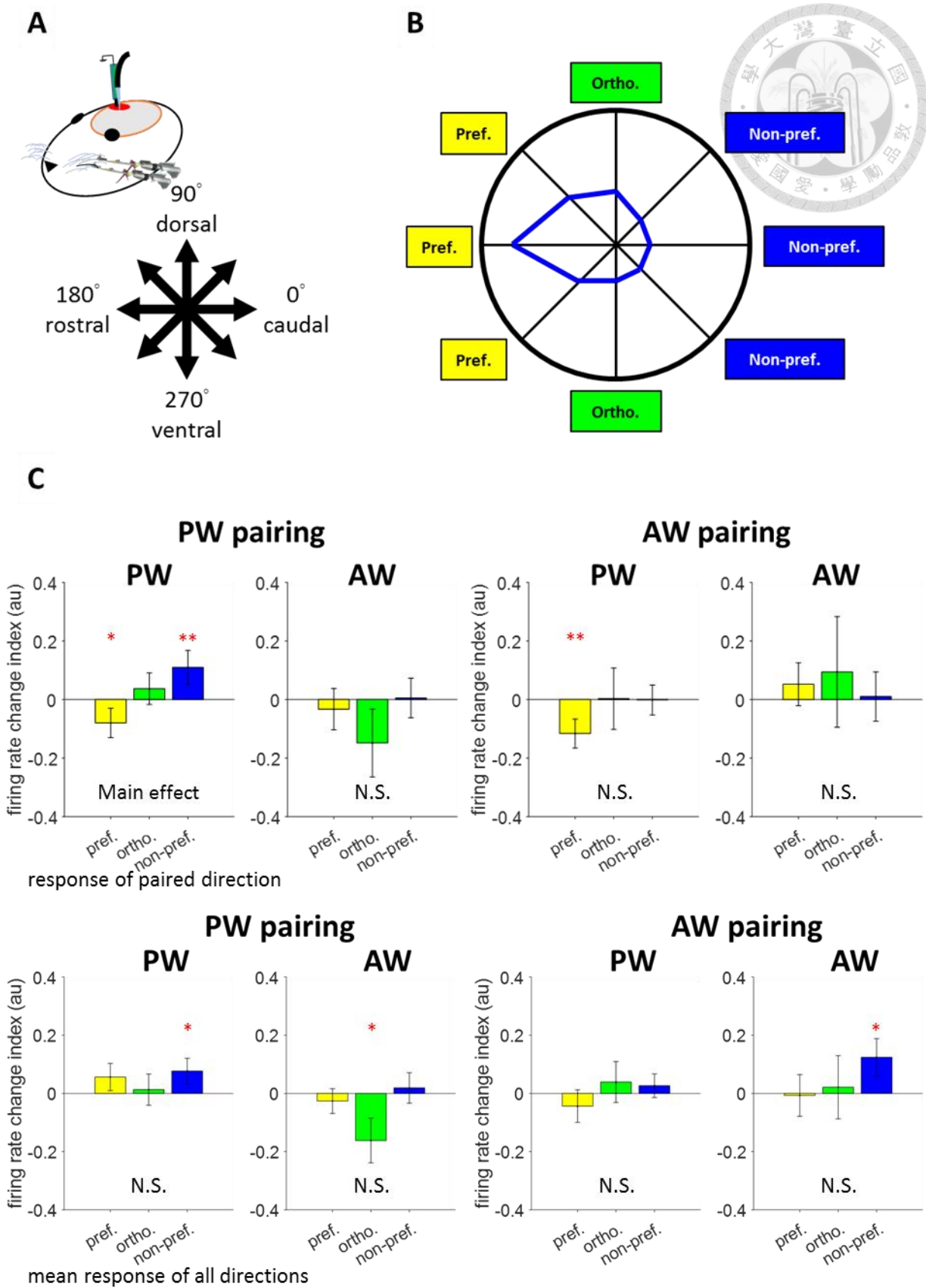of paired direction. Similar results are observed in response of paired direction.

Figure 11. Results of manipulations based on neurons' direction selectivity.
A. Scheme of whisker deflection directions. There are 8 deflection direction along

vertical and horizontal axes and intermedium angles: 0° for caudal and 180° for rostral, 90° for dorsal and 270° for ventral. **B.** Categorization criteria. Blue line indicates schematic direction selectivity of a neuron, with preference of physical stimulus in 180°. The criteria is as follow: group 1 (preferred): neurons receive pairings of physical stimulus in preferred direction or preferred direction ± 45°; group 2 (orthogonal): neurons receive pairings of physical stimulus in orthogonal direction relative to preferred direction; group 3 (non-preferred): neurons receive pairings of physical stimulus in non-preferred directions. **C.** Top: firing rate change index of the response in paired direction versus paired direction. Bottom: firing rate change index of the mean response for all directions versus paired direction. Red markers indicate significances of firing rate change index using Wilcoxon rank sum test, * for p < .05 and ** for p < .01.
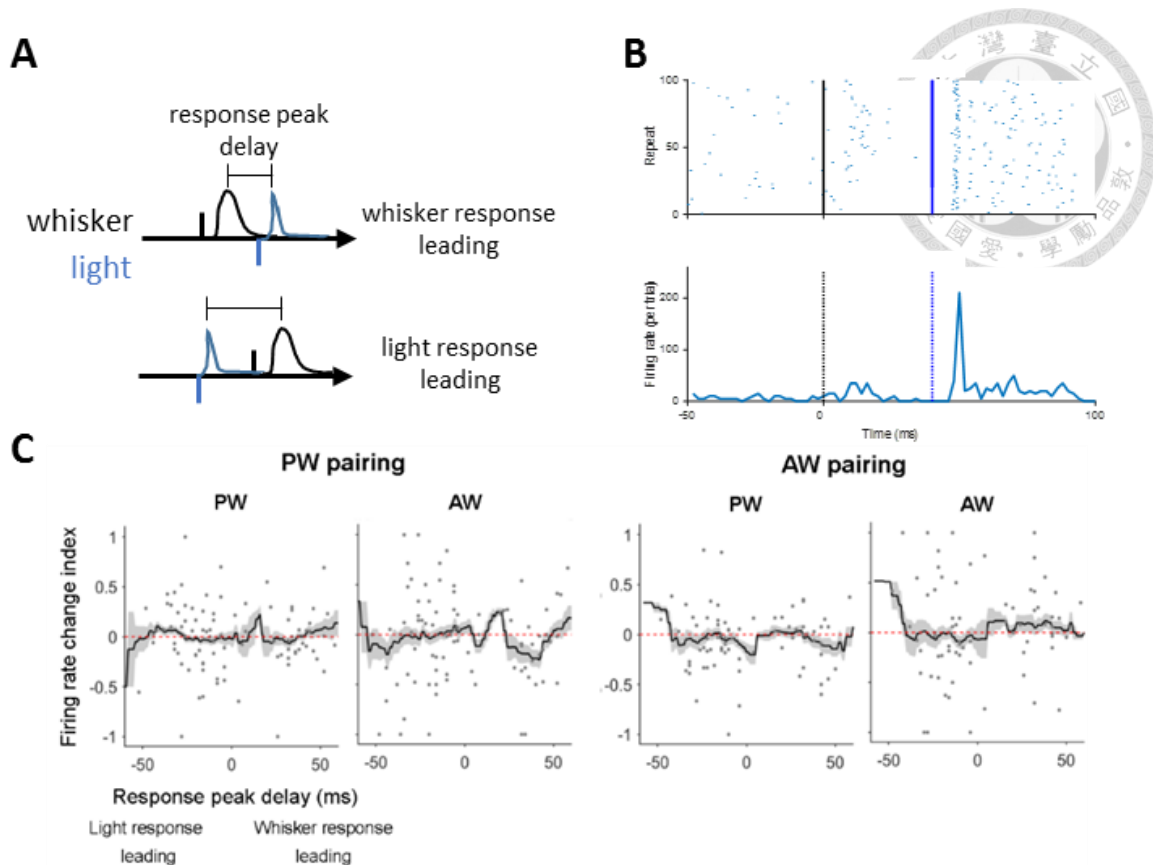
Figure 12. Neuronal activity changes under different SOAs.
A. Scheme of response peak delay calculation. **B.** Raster plot and PSTH for an example
unit during pairing. Black solid line in raster plot and black dashed line in PSTH are
timing of physical stimulus onset. Blue solid line in raster plot and blue dashed line in
PSTH are timing of light stimulus onset **C.** Firing rate change index of paired direction
versus response peak delay between physical evoked response and light evoked response
during pairing session. No significant time window is detected using Wilcoxon rank sum
test. Black line indicates sliding average with 20 ms width and 1 ms step. Gray area
indicates standard error of mean of each sliding window. Red dashed line indicates 0 of y
axis.
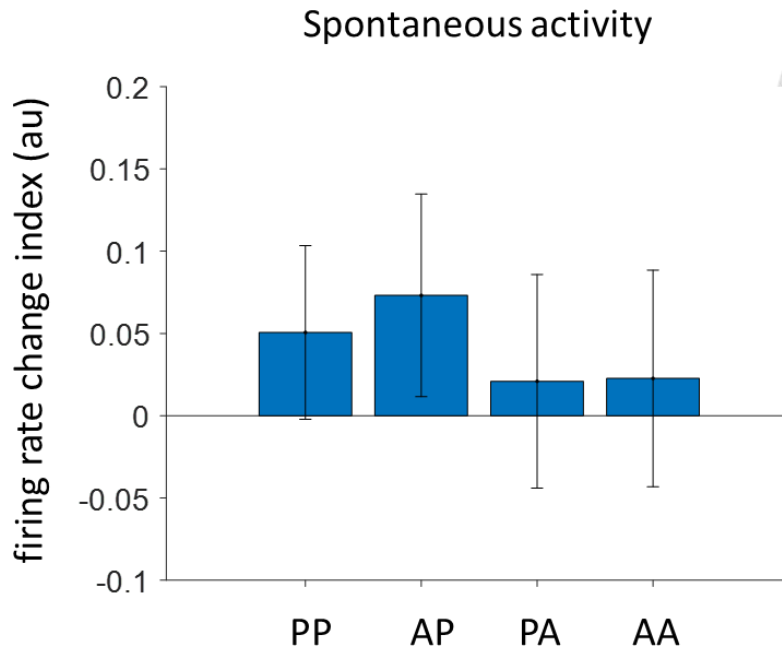
Figure 13. Change of spontaneous activity after pairing.
Firing rate change index of baseline is calculated for PW and AW responses under PW-pairing and AW-pairing conditions. PP, AP are the abbreviations of PW responses under PW-pairing condition and AW responses under PW-pairing condition, respectively. PA, AA are the abbreviations of PW responses under AW-pairing condition and AW responses under AW-pairing condition, respectively.

41

Figure 14. Change of direction selectivity.
A. Example of direction selectivity change. Left: angular difference between preferred direction and paired direction for each unit, before pairing versus after pairing. Right: a

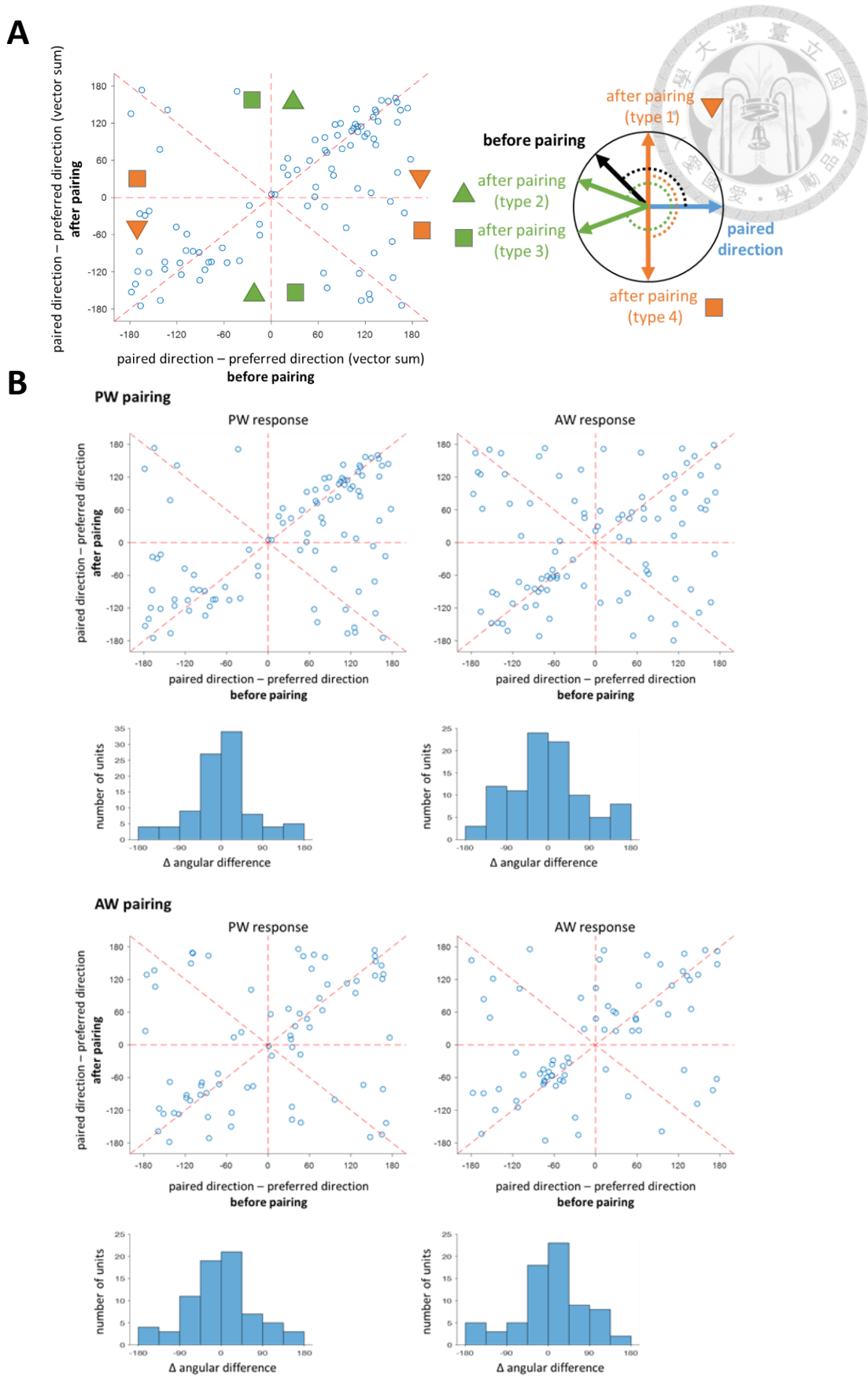scheme of angular difference between preferred direction and paired direction. Preferred direction here is the direction of vector summation of neuronal response in each deflection direction. Black arrow indicates the preferred direction before pairing. Blue arrow indicates the paired direction in pairings. Orange markers indicate decreased angular difference after pairing. Green markers indicate increased angular difference after pairing. Triangle markers indicate angular difference from paired direction is less than 180°. Square markers indicate angular difference from paired direction is more than 180°.
B. Angular difference before pairing versus angular difference after pairing and distribution the change. Below each scatter plot is a histogram manifested the distribution of △ angular differences, which are the results of x-axis values subtract y-axis values in the scatter plot.
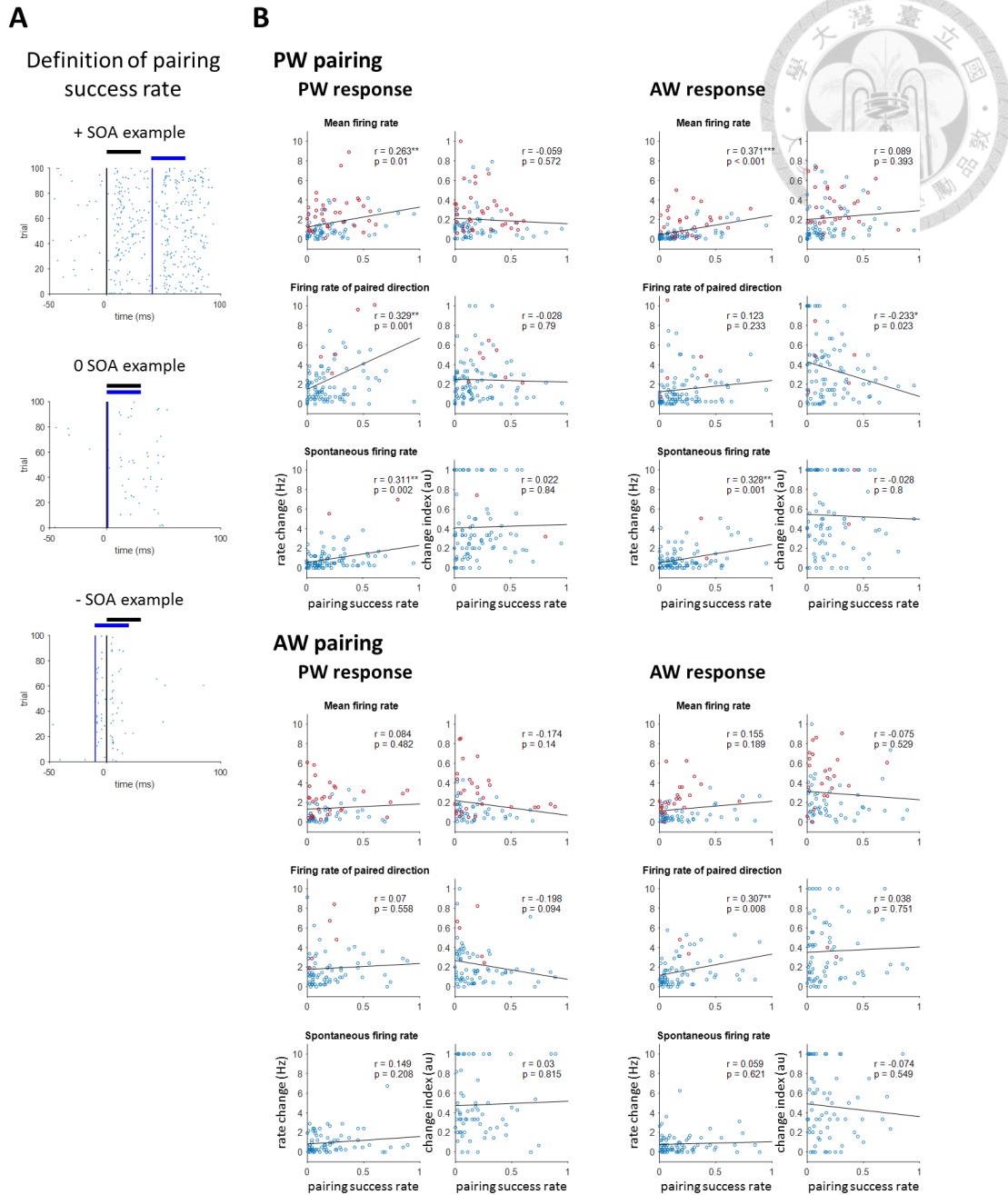
43

Figure 15. Pairing success rate versus neural activity change.
A. Definition and PSTH examples of pairing success rate. In pairings, when there is at least one spike within 30-ms time window after stimulus onset for both optical and physical stimulus, the trial is considered as a success pair. Blue solid line indicates optical stimulus onset. Black solid line indicates physical stimulus onset. Blue short lines indicate spike timing. **B.** Correlation between magnitude of pairing success rate and absolute values of magnitude of neural activity change. Magnitude of neural activity change is demonstrated in absolute values in order to estimate whether activity change is related to pairing success rate. Pairing success rate is defined as the ratio of trials which optical evoked spike and physical evoked spike are observed in pairing session. Black line indicates the least-squares line of data in each subfigure. Red markers indicate units whose neural activity significantly changed.

Table 2
Results of Stepwise Multiple Linear Regression

Dependent variable	Formula	Adjusted R-squared
Firing rate change of preferred direction	1 + Pairing type*Firing probability + Peak delay*Firing probability	0.193
Mean firing rate change	1 + Whisker ID + Paired direction + Pairing type*Firing probability	0.104
Firing rate change of paired direction	1 + Firing probability + Whisker ID*Paired direction	0.077
Mean firing rate change index	1 + Firing probability + Whisker ID*Pairing type	0.058
Spontaneous firing rate change	1 + Firing probability	0.019
Spontaneous firing rate change index	1 + Peak delay	0.015
Firing rate change index of paired direction	1 + Paired direction	0.006
Firing rate change index of preferred direction	1	0

Note. Firing rate change and firing rate change index are the responses for regression models. A constant (written as 1 in formula), Whisker ID (PW response or AW response), Pairing type (PW pairing or AW pairing), Firing probability, Paired direction, Peak delay and their interaction terms (one-on-one, denoted by A*B) are the predictors for regression models.

Table 3

Predictors and Coefficients for Each Stepwise Multiple Linear Regression Model

Firing rate change of preferred direction

Independent variable	Coefficient	p value
(Intercept)	0.081	.854
Pairing type	1.841	.007
Peak delay	0.026	.015
Firing probability	-3.619	.001
Pairing type* Firing probability	-5.831	< .001
Peak delay* Firing probability	-0.075	.004

Mean firing rate change index

Independent variable	Coefficient	p value
(Intercept)	0.213	< .001
Whisker ID	-0.134	.003
Pairing type	-0.072	.123
Firing probability	-0.365	< .001
Whisker ID* Pairing type	0.167	.012

Mean firing rate change

Independent variable	Coefficient	p value
(Intercept)	0.450	.232
Whisker ID	-0.377	.065
Pairing type	0.745	.076
Paired direction	0.190	.087
Firing probability	-1.746	.007
Pairing type* Firing probability	-2.608	.010

Spontaneous firing rate change

Independent variable	Coefficient	p value
(Intercept)	0.458	.005
Firing probability	-1.049	.007

Spontaneous firing rate change index

Independent variable	Coefficient	p value
(Intercept)	0.052	.117
Peak delay	-0.030	.017

Firing rate change of paired direction

Independent variable	Coefficient	p value
(Intercept)	-1.212	.056
Whisker ID	2.117	.005
Paired direction	1.034	< .001
Firing probability	-2.752	.001
Whisker ID* Paired direction	-1.122	.001

Firing rate change index of paired direction

Independent variable	Coefficient	p value
(Intercept)	-0.096	.063
Paired direction	0.043	.079

Firing rate change index of preferred direction

Independent variable	Coefficient	p value
(Intercept)	-0.137	< .001

Note. Predictors and their corresponding coefficients for models in Table 2.

4. Discussion
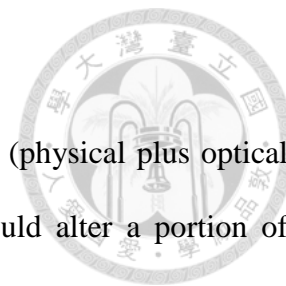
In this study, we found that the stimulus pairing paradigm (physical plus optical stimulation), which was widely used in many STDP studies, could alter a portion of excitatory neurons *in vivo* in the adult rat barrel cortex. This magnitude of induced neuroplasticity was determined by intrinsic neuronal properties such as firing probability and preferred direction, but not related to the timing between physical and optical stimulations. While the optogenetic tool was an effective tool to induce neuroplasticity by stimulating a large neuronal population in the barrel cortex, the STDP rule was not followed in this case.

4.1. Manipulation on Discrete Pathways Resulted in Different Pattern

Present study showed that pairing adjacent whisker (AW) with optical stimulation would also influence the evoked neuronal activity of the principal whisker (PW) (Figs. 8-10). These results indicated that tactile information from multiple whiskers was likely integrated in barrel cortex. Meliza and Dan (2006) reported similar results that neuronal activity evoked by different input pathways or by different stimulus features would affect responses coming from other pathways projected to the same neuron. They found that the receptive field of rodent V1 neurons changed after the STDP protocol. Neuronal activity induced by stimulation placed at either the neighboring site or an even farther one might also change as that in the paired site did.

However, some studies had reported opposite results: there was no influence caused by the manipulation of the neighboring whisker projecting to the same neuron. Jacob et al (2007) found that only the paired whisker showed plasticity (firing rate and postsynaptic potential change) after the STDP protocol. The activity induced by the unpaired whisker did not change before and after the pairing. Katz et al. (2006) also found that the adaptation
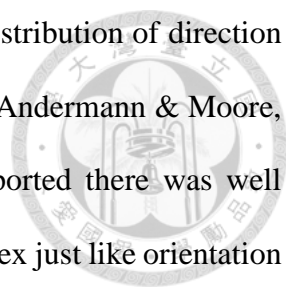
performed on one whisker would not influence subsequent neuronal response evoked by a neighboring whisker in barrel. The main difference between these previous studies and our study was the magnitude of the paired stimulation. Previous studies used current injection as the stimulation, which might affect a small number of neurons. In contrast, our study used optogenetic tool as the stimulation, which might affect a large population of neurons. Expression of channelrhodopsin might also alter neuronal functions and their response properties to physical stimulation.

There could be two possibilities to further explain our results: synapses carrying PW information were close to synapses carrying AW information so they were both influenced by pairing manipulation, or the change of manipulated synapse would alter intracellular mechanism which end up influence synapses carrying the non-manipulated whisker's signal. Thus, the synaptic weight of each whisker changed simultaneously after the pairing of optical and physical stimuli.

We also found that the influence on neighboring whisker was different between the manipulations of PW and AW. Though PW manipulation might change a portion of neuron's AW evoked firing rate, they had little influence on AW evoked activity properties (Fig. 10B-C, 11C), which might somehow congruent with result in study of Jacob et al in 2007. On the other hand, AW manipulation tended to suppress PW evoked activity (Fig. 10B-C, 11C). This result indicated an unbalanced cross-whisker influence mechanism might lead to suppress highly active responses.

4.2. Result of Preferred Stimulus Feature Might Imply the Formation of Directional Selectivity (or the Changeability of Its Weightings)

Neurons in rodent whisker-barrel system were reported to show direction selectivity along its projection from thalamus to cortex. There were many studies attempted

to address the formation and distribution of direction selectivity. Distribution of direction selectivity in barrel cortex is a contentious issue, some researches (Andermann & Moore, 2006; Kremer, Leger, Goodman, Brette, & Bourdieu, 2011) supported there was well organized direction selectivity map in the rodent somatosensory cortex just like orientation pinwheels in primate primary visual cortex, while others (Bruno, Khatri, Land, & Simons, 2003) supported direction selectivity of rodent S1 abruptly changed in short spatial distances. The study suggested that there were minicolumns inside the barrel columns, with vertical circuit connecting different layers, neurons within a minicolumn showed similar direction selectivity. However, there was abrupt change of direction selectivity when recording horizontally adjacent sites (Bruno et al., 2003). For the formation of direction selectivity, there were also various hypothesis: thalamocortical neurons with similar direction selectivity projected to similar position in barrel columns (Bruno et al., 2003), nonlinearity dendritic processing of angular information determined selectivity of layer IV spiny stellate neurons (Lavzin, Rapoport, Polsky, Garion, & Schiller, 2012), and separated thalamocortical projection of angular information to corresponding position in barrel column which might also fit relative position on topographic map of whisker identity (Andermann & Moore, 2006; L. Li & Ebner, 2007).

Our data showed that when the manipulation was made on a specific deflection direction, the preference of the paired direction had a main effect on the change of evoked response for whisker stimulation in the paired direction. This result indicated that circuits carrying direction selectivity information to sensory neurons in barrel column might be separated for each direction. Also, circuits carrying specific angular preference might project to several neighboring barrel columns near their principal barrel columns. Our results (Fig. 11C) might somehow support the hypothesis (Andermann & Moore, 2006; L. Li & Ebner, 2007) of independently transmitted angular information but not sufficient to

49

verify the distribution of direction selectivity in somatosensory cortex.
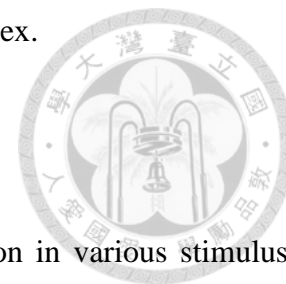
4.3. Lack of Timing Effect

We paired optogenetic stimulation and physical stimulation in various stimulus onset asynchronies (SOAs), and to our surprise there was no timing effect. The change in neuronal activity was not related to the SOA or delay of evoked response latencies (Fig. 12C). The discrepancy between present results and previous studies about STDP rule might be caused by the usage of optogenetic tool *in vivo*, since light stimulation was delivered through optical fiber stub, which illuminated the recording site and might activate a population of infected neurons at once rather than selectively manipulating one postsynaptic neuron a time. In other words, our light stimulation was not spatially specific enough.

Most studies of STDP (Feldman, 2012) measured postsynaptic potential (PSP) changes via *in vitro* patch-clamp recordings in brain slices. They had good vision of their paired presynaptic and postsynaptic neurons under microscopes, and specifically discharged neurons with current injection into patched cells. Few studies used similar patch-clamp recording method (Jacob et al., 2007; Meliza & Dan, 2006) under *in vivo* condition might lose their precision on controlling presynaptic input because they used physical stimulation, which might be vulnerable to miss or misalignment of sensory input along the sensory pathway from receptors in peripheral to sensory cortex in the brain (Lube, 2019). However, they reported similar results of with previous *in vitro* studies. Jacob et al (2007) even showed that their data recorded at action potential level was congruent with the STDP studies recorded at the PSP level. Thus, difference in recording methods might not be the reason why we observed no timing effect.

Another possible reason for no timing effect with the optogenetic tool was that the

channelrhodopsin was an exogenous ion channel for neurons. Cation influx caused by light stimulation through channelrhodopsin might not induce similar molecular reaction cascades with cation influx caused by electrical stimulation which opened endogenous voltage sensitive channels.
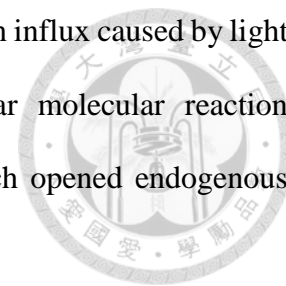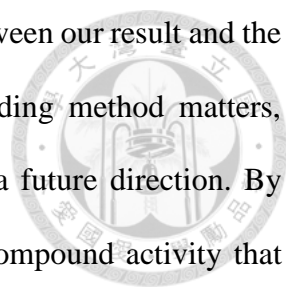
Last but not least, our estimation of neuronal activity timing was based on action potentials extracellularly recorded, which was not the canonical measurement in STDP protocols. In most *in vitro* STDP studies, researchers defined spike timing between the initial of postsynaptic EPSP and the peak of action potential evoked by current injection (Jacob et al., 2007; Feldman, 2012). Maybe we should improve our electrophysiology recording system to simultaneously perform membrane potential and action potential recordings, so that we could verify whether timing effect truly play no role under our manipulation.

4.4. Limitation of Present Study & Future Directions

In this study, we focused on neuroplasticity of a large number of cortical neurons in an *in-vivo* condition. We found that using the STDP protocol we could induce functional plasticity in a portion of neurons. We also could not verify the underling cellular mechanism with our experimental design. Advanced study of better spatial control of light stimulation or usage of channel blocker, such as antagonists like AP5, would help us construct some knowledge about the detailed neuronal mechanism. With the whole picture of optogenetic-physical stimulus induced neuroplasticity, it might shed light on future works attempting to perform large scale cortical function reorganization or cortical function rehabilitation after brain injuries.
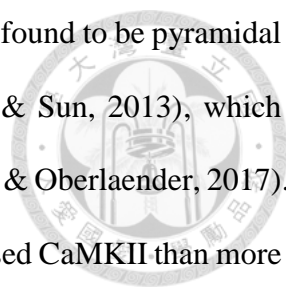
Firstly, our results were based on single-unit extracellular recordings of action potentials, which had been proved to be highly correlated to PSP changes (Knox, 1974;

51

Knox & Poppele, 1977), might still be a reason of incongruence between our result and the STDP rule. If we would like to address whether different recording method matters, performing simultaneous intra-/extracellular recordings might be a future direction. By doing this, we could also verify whether light stimulus induced compound activity that could still be detected in intracellular recordings. If there was no overwhelming compound activity under intracellular recording settings, we could better measure light evoked activities. Accordingly, we might get data with better quality. Another possible future direction in electrophysiology recordings is performing the LFP analysis, which might reveal information of population processing (Bessaih, Higley, & Contreras, 2018; Shin & Moore, 2019) in the barrel field. For instance, through spectrum analysis of the LFP, we could monitor power of several frequency bands to address the question that whether neuronal activity of the entire recorded area changed after manipulation or only a few cells had their activity changed with others unchanged.

Secondly, pairing success rate in present study might not faithfully represent success pairs described in STDP protocols because our estimation was based on action potential evoked by presynaptic neuron (physical stimulus), and action potential directly induced by optical stimulus but not EPSP and action potential. Even if our estimation of pairing success rate was suitable, it was low for most units, especially when physical stimulus was not on the PW and in the optimal direction. An additional measurement of membrane potential change or a larger number of pairing trials should be applied to better quantify how well our manipulation is and how much pairs was sufficient to induce neuroplasticity in this case.

Last but not least, we infected CaMKII expressing neurons with an AAV vector, and recorded neuronal activity, induced neuroplasticity from units which could be driven by light stimulation. However, we did not strictly define in which cortical layer we made our

recordings. Most neurons expressing CaMKII in the neocortex were found to be pyramidal cells (E. Jones, Huntley, & Benson, 1994; Wang, Zhang, Szabo, & Sun, 2013), which distributed mostly in layer II/III and layer V/VI (Narayanan, Udvary, & Oberlaender, 2017). It has been reported that pyramidal cells in layer II/III and VI expressed CaMKII than more robustly those in other cortical layers (Wang et al., 2013). In present study, we performed electrophysiology recordings at 1.10 ± 0.04 mm depth from cortical surface of rats, which might be the upper layer V, but we did not perform Nissl stain or CO stain to verify the cortical depth. In future study, we should take laminar specificity into consideration in order to better understand which cortical layer is more sensitive to the manipulation of neuroplasticity. We could not only learn what role each layer plays but also what degree neurons in different layers can be guided.

4.5. Possible Future Choices of Parameters & Conditions

Based on present experimental setups, we will possibly carry on studies with new design and alternative parameters and conditions. To improve spatial resolution of optical stimulation, we can decrease the volume or titer of the virus injection. Furthermore, we can testify how to limit the illumination area so as to achieve locally turn on channelrhodopsin rather than activate the whole circuits. We are also interested in the relationship between wakefulness and neuroplasticity. Though it might be more complicate in the awake brain, it is still the most representative scenario to understand how living animals learn or develop in their daily lives.

References

Andermann, M. L., & Moore, C. I. (2006). A somatotopic map of vibrissa motion direction within a barrel column. *Nature Neuroscience, 9*, 543-551. doi:10.1038/nn1671

Aravanis, A. M., Wang, L. P., Zhang, F., Meltzer, L. A., Mogri, M. Z., Schneider, M. B., & Deisseroth, K. (2007). An optical neural interface: in vivo control of rodent motor cortex with integrated fiberoptic and optogenetic technology. *Journal of Neural Engineering, 4*, S143-156. doi:10.1088/1741-2560/4/3/S02

Bessaih, T., Higley, M. J., & Contreras, D. (2018). Millisecond precision temporal encoding of stimulus features during cortically generated gamma oscillations in the rat somatosensory cortex. *Journal of Physiology, 596*, 515-534. doi:10.1113/JP275245

Bi, G. Q., & Poo, M. M. (1998). Synaptic modifications in cultured hippocampal neurons: dependence on spike timing, synaptic strength, and postsynaptic cell type. *Journal of Neuroscience, 18*, 10464-10472.

Bruno, R. M., Khatri, V., Land, P. W., & Simons, D. J. (2003). Thalamocortical angular tuning domains within individual barrels of rat somatosensory cortex. *Journal of Neuroscience, 23*, 9565-9574.

Butts, D. A., Weng, C., Jin, J., Yeh, C. I., Lesica, N. A., Alonso, J. M., & Stanley, G. B. (2007). Temporal precision in the neural code and the timescales of natural vision. *Nature, 449*, 92-95. doi:10.1038/nature06105

de Kock, C. P., Bruno, R. M., Spors, H., & Sakmann, B. (2007). Layer- and cell-type-specific suprathreshold stimulus representation in rat primary somatosensory cortex. *Journal of Physiology, 581*, 139-154. doi:10.1113/jphysiol.2006.124321

Engel, A. K., König, P., Kreiter, A. K., Schillen, T. B., & Singer, W. (1992). Temporal

coding in the visual cortex: new vistas on integration in the nervous system. *Trends in Neurosciences, 15*, 218-226.
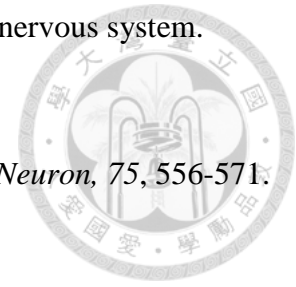
Feldman, D. E. (2012). The spike-timing dependence of plasticity. *Neuron, 75*, 556-571. doi:10.1016/j.neuron.2012.08.001

Feldman, D. E., & Brecht, M. (2005). Map plasticity in somatosensory cortex. *Science, 310*, 810-815.

Gunaydin, L. A., Yizhar, O., Berndt, A., Sohal, V. S., Deisseroth, K., & Hegemann, P. (2010). Ultrafast optogenetic control. *Nature Neuroscience, 13*, 387-392. doi:10.1038/nn.2495

Hebb, D. (1949). *The organization of behavior* (Vol. 65). New York: Wiley.

Heiss, J. E., Katz, Y., Ganmor, E., & Lampl, I. (2008). Shift in the balance between excitation and inhibition during sensory adaptation of S1 neurons. *Journal of Neuroscience, 28*, 13320-13330. doi:10.1523/JNEUROSCI.2646-08.2008

Jacob, V., Brasier, D. J., Erchova, I., Feldman, D., & Shulz, D. E. (2007). Spike timing-dependent synaptic depression in the in vivo barrel cortex of the rat. *Journal of Neuroscience, 27*, 1271-1284. doi:10.1523/JNEUROSCI.4264-06.2007

Jacob, V., Mitani, A., Toyoizumi, T., & Fox, K. (2017). Whisker row deprivation affects the flow of sensory information through rat barrel cortex. *Journal of Neurophysiology, 117*, 4-17. doi:10.1152/jn.00289.2016

Jacob, V., Petreanu, L., Wright, N., Svoboda, K., & Fox, K. (2012). Regular spiking and intrinsic bursting pyramidal cells show orthogonal forms of experience-dependent plasticity in layer V of barrel cortex. *Neuron, 73*, 391-404. doi:10.1016/j.neuron.2011.11.034

Jones, E., Huntley, G., & Benson, D. (1994). Alpha calcium/calmodulin-dependent protein kinase II selectively expressed in a subpopulation of excitatory neurons in

monkey sensory-motor cortex: comparison with GAD-67 expression. *Journal of Neuroscience, 14*, 611-629.
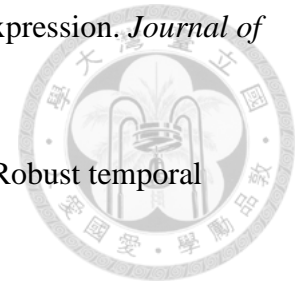
Jones, L. M., Depireux, D. A., Simons, D. J., & Keller, A. (2004). Robust temporal coding in the trigeminal system. *Science, 304*, 1986-1989.

Katz, Y., Heiss, J. E., & Lampl, I. (2006). Cross-whisker adaptation of neurons in the rat barrel cortex. *Journal of Neuroscience, 26*, 13363-13372. doi:10.1523/JNEUROSCI.4056-06.2006

Khatri, V., Hartings, J. A., & Simons, D. J. (2004). Adaptation in thalamic barreloid and cortical barrel neurons to periodic whisker deflections varying in frequency and velocity. *Journal of Neurophysiology, 92*, 3244-3254. doi:10.1152/jn.00257.2004

Khatri, V., & Simons, D. J. (2007). Angularly nonspecific response suppression in rat barrel cortex. *Cerebral Cortex, 17*, 599-609. doi:10.1093/cercor/bhk006

Knox, C. (1974). Cross-correlation functions for a neuronal model. *Biophysical Journal, 14*, 567-582.

Knox, C., & Poppele, R. (1977). Correlation analysis of stimulus-evoked changes in excitability of spontaneously firing neurons. *Journal of Neurophysiology, 40*, 616-625.

Kremer, Y., Leger, J. F., Goodman, D., Brette, R., & Bourdieu, L. (2011). Late emergence of the vibrissa direction selectivity map in the rat barrel cortex. *Journal of Neuroscience, 31*, 10689-10700. doi:10.1523/JNEUROSCI.6541-10.2011

Lavzin, M., Rapoport, S., Polsky, A., Garion, L., & Schiller, J. (2012). Nonlinear dendritic processing determines angular tuning of barrel cortex neurons in vivo. *Nature, 490*, 397-401. doi:10.1038/nature11451

Le Cam, J., Estebanez, L., Jacob, V., & Shulz, D. E. (2011). Spatial structure of

multiwhisker receptive fields in the barrel cortex is stimulus dependent. *Journal of Neurophysiology, 106*, 986-998. doi:10.1152/jn.00044.2011

Li, L., & Ebner, F. F. (2007). Cortical modulation of spatial and angular tuning maps in the rat thalamus. *Journal of Neuroscience, 27*, 167-179. doi:10.1523/JNEUROSCI.4165-06.2007

Li, N., Downey, J. E., Bar-Shir, A., Gilad, A. A., Walczak, P., Kim, H., . . . Pelled, G. (2011). Optogenetic-guided cortical plasticity after nerve injury. *Proceedings of the National Academy of Sciences, 108*, 8838-8843. doi:10.1073/pnas.1100815108

Lube A. J., M. X., Carlson B. A. (2019). *Spike-timing-dependent plasticity alters sensory network connectivity in vivo.* Poster presented at the Neuroscience 2019, Chicago.

Maravall, M., Petersen, R. S., Fairhall, A. L., Arabzadeh, E., & Diamond, M. E. (2007). Shifts in coding properties and maintenance of information transmission during adaptation in barrel cortex. *PLoS Biology, 5*, e19. doi:10.1371/journal.pbio.0050019

Meliza, C. D., & Dan, Y. (2006). Receptive-field modification in rat visual cortex induced by paired visual stimulation and single-cell spiking. *Neuron, 49*, 183-189. doi:10.1016/j.neuron.2005.12.009

Narayanan, R. T., Udvary, D., & Oberlaender, M. (2017). Cell Type-Specific Structural Organization of the Six Layers in Rat Barrel Cortex. *Frontiers in Neuroanatomy, 11*, 91. doi:10.3389/fnana.2017.00091

Petersen, C. C. (2007). The functional organization of the barrel cortex. *Neuron, 56*, 339-355. doi:10.1016/j.neuron.2007.09.017

Petersen, C. C., Hahn, T. T., Mehta, M., Grinvald, A., & Sakmann, B. (2003). Interaction of sensory responses with spontaneous depolarization in layer 2/3 barrel cortex.

Proceedings of the National Academy of Sciences, 100, 13638-13643.

Rasmusson, D. D. (1982). Reorganization of raccoon somatosensory cortex following removal of the fifth digit. *Journal of Comparative Neurology, 205*, 313-326.

Shin, H., & Moore, C. I. (2019). Persistent Gamma Spiking in SI Nonsensory Fast Spiking Cells Predicts Perceptual Success. *Neuron, 103*, 1150-1163 e1155. doi:10.1016/j.neuron.2019.06.014

Simons, D. J. (1978). Response properties of vibrissa units in rat SI somatosensory neocortex. *Journal of Neurophysiology, 41*, 798-820.

Simons, D. J. (1983). Multi-whisker stimulation and its effects on vibrissa units in rat Sml barrel cortex. *Brain Research, 276*, 178-182.

Singh, C., & Levy, W. B. (2017). A consensus layer V pyramidal neuron can sustain interpulse-interval coding. *PLoS One, 12*, e0180839. doi:10.1371/journal.pone.0180839

Van der Loos, H., & Woolsey, T. A. (1973). Somatosensory cortex: structural alterations following early injury to sense organs. *Science, 179*, 395-398.

Wang, X., Zhang, C., Szabo, G., & Sun, Q. Q. (2013). Distribution of CaMKIIalpha expression in the brain in vivo, studied by CaMKIIalpha-GFP mice. *Brain Research, 1518*, 9-25. doi:10.1016/j.brainres.2013.04.042

Woolsey, T. A., & Van der Loos, H. (1970). The structural organization of layer IV in the somatosensory region (SI) of mouse cerebral cortex: the description of a cortical field composed of discrete cytoarchitectonic units. *Brain Research, 17*, 205-242.

Wright, N., & Fox, K. (2010). Origins of cortical layer V surround receptive fields in the rat barrel cortex. *Journal of Neurophysiology, 103*, 709-724. doi:10.1152/jn.00560.2009

Yao, H., & Dan, Y. (2001). Stimulus timing-dependent plasticity in cortical processing of

orientation. *Neuron, 32*, 315-323.

Zhao, S., Ting, J. T., Atallah, H. E., Qiu, L., Tan, J., Gloss, B., . . . Feng, G. (2011). Cell type-specific channelrhodopsin-2 transgenic mice for optogenetic dissection of neural circuitry function. *Nature Methods, 8*, 745-752. doi:10.1038/nmeth.1668